



FULL PAPER

Discovery and antiproliferative evaluation of new quinoxalines as potential DNA intercalators and topoisomerase II inhibitors

Ibrahim H. Eissa¹ | Ahmed M. Metwaly² | Amany Belal^{3,4} | Ahmed B.M. Mehany⁵ | Rezk R. Ayyad¹ | Khaled El-Adl^{1,6} | Hazem A. Mahdy¹ | Mohammed S. Taghour¹ | Kamal M.A. El-Gamal⁷ | Mohamad E. El-Sawah⁷ | Souad A. Elmetwally⁸ | Mostafa. A. Elhendawy⁹ | Mohamed M. Radwan^{9,10} | Mahmoud A. ElSohly^{9,11}

¹Pharmaceutical Medicinal Chemistry Department, Faculty of Pharmacy (Boys), Al-Azhar University, Cairo, Egypt

²Department of Pharmacognosy, Faculty of Pharmacy (Boys), Al-Azhar University, Cairo, Egypt

³Department of Medicinal Chemistry, Faculty of Pharmacy, Beni-Suef University, Beni-Suef, Egypt

⁴Department of Pharmaceutical Chemistry, College of Pharmacy, Taif University, Taif, Saudi Arabia

⁵Department of Zoology, Faculty of Science, Al-Azhar University, Cairo, Egypt

⁶Department of Pharmaceutical Chemistry, Faculty of Pharmacy and Drug Technology, Heliopolis University for Sustainable Development, Cairo, Egypt

⁷Department of Pharmaceutical Organic Chemistry, Faculty of Pharmacy (Boys), Al-Azhar University, Cairo, Egypt

⁸Department of Basic Science, Higher Technological Institute, 10th of Ramadan City, Egypt

⁹National Center for Natural Products Research, University of Mississippi, Mississippi

¹⁰Department of Pharmacognosy, Faculty of Pharmacy, Alexandria University, Alexandria, Egypt

¹¹Department of Pharmaceutics and Drug Delivery, University of Mississippi, Mississippi, Mississippi

Correspondence

Ibrahim H. Eissa, Pharmaceutical Medicinal Chemistry Department, Faculty of Pharmacy (Boys), Al-Azhar University, Cairo 11884, Egypt.

Email: Ibrahim.eissa@azhar.edu.eg

Mahmoud A. ElSohly, National Center for Natural Products Research, University of Mississippi, MS 38677, USA.

Email: mmelsohly@olemiss.edu

Abstract

In continuation of our previous work on the design and synthesis of topoisomerase II (Topo II) inhibitors and DNA intercalators, a new series of quinoxaline derivatives were designed and synthesized. The synthesized compounds were evaluated for their cytotoxic activities against a panel of three cancer cell lines (Hep G-2, Hep-2, and Caco-2). Compounds **18b**, **19b**, **23**, **25b**, and **26** showed strong potencies against all tested cell lines with IC₅₀ values ranging from 0.26 ± 0.1 to 2.91 ± 0.1 μM, comparable with those of doxorubicin (IC₅₀ values ranging from 0.65 ± 0.1 to 0.81 ± 0.1 μM). The most active compounds were further evaluated for their Topo II inhibitory activities and DNA intercalating affinities. Compounds **19b** and **19c** exhibited high activities against Topo II (IC₅₀ = 0.97 ± 0.1 and 1.10 ± 0.1 μM, respectively) and bound the DNA at concentrations of 43.51 ± 2.0 and 49.11 ± 1.8 μM, respectively, whereas compound **28b** exhibited a significant affinity to bind the DNA with an IC₅₀ value of 37.06 ± 1.8 μM. Moreover, apoptosis and cell-cycle tests of the most promising compound **19b** were carried out. It was found that **19b** can significantly induce apoptosis in Hep G-2 cells. It has revealed cell-cycle arrest at the G2/M phase. Moreover, compound **19b** downregulated the Bcl-2 levels, indicating its potential to enhance apoptosis. Furthermore, molecular docking studies were carried out against the DNA–Topo II complex to examine the binding patterns of the synthesized compounds.

KEYWORDS

anticancer, apoptosis, DNA intercalator, molecular docking, quinoxalines, topoisomerase II

1 | INTRODUCTION

According to the WHO fact sheet, published in October 2018, cancer is the second leading cause of death all over the world, accounting for 9.6 million deaths in 2018. The number of affected persons over the next 20 years is expected to increase by around 70%.^[1] Anticancer drugs have been classified into two types: the first one is drugs that affect DNA, RNA, or proteins. The second target includes other elements involved in the carcinogenesis process, such as the immune system, the endothelium, and the extracellular matrix.^[2] Molecules that affect DNA include groove binders, alkylating agents, DNA intercalators, and topoisomerase inhibitors.^[3]

Topoisomerases are important nuclear enzymes, which play a crucial role in DNA replication, transcription, chromosome segregation, and recombination.^[4] There are two major types of topoisomerases. (a) Topoisomerase I (Topo I), which is responsible for cleavage, relaxing, and releasing of one strand of the DNA duplex. (b) Topoisomerase II (Topo II), which cleaves both strands of the DNA helix simultaneously to remove DNA supercoiling.^[5] These enzymes covalently bind to DNA via tyrosine residues in the active site. These linkages are transient and easily reversible, and the covalently bound structure is known as the cleavable complex.^[6] Accordingly, topoisomerases are considered as important targets for cancer chemotherapy treatments.^[7] Topoisomerase inhibitors block the ligation step of the cell-cycle, generating single- and double-stranded breaks that harm the integrity of the genome.^[8] Introduction of these breaks subsequently leads to apoptosis and cell death.^[9]

Some anticancer drugs targeting Topo II inhibit the enzymatic activity as a primary mode of action and are known as catalytic Topo II inhibitors.^[10] Another type of Topo II-targeting drugs, including intercalating drugs, interfere with the enzyme's cleavage and rejoining activities by trapping the cleavable complex and thereby increasing the half-life of the transient Topo II-catalyzed DNA breaks. These drugs are referred to as Topo II poisons because they convert the Topo II enzyme into a DNA-damaging agent.^[7,10]

DNA intercalators as Topo II poisons are molecules that intercalate between DNA base pairs. They have attracted particular attention due to their promising antitumor activities.^[11] Many intercalative Topo II poisons are either used already as anticancer drugs or still under clinical trials (e.g., doxorubicin **1**,^[12] amsacrine **3**,^[13] mitoxantrone **2**,^[14] ellipticine **4**,^[15] and nogalamycin **5**^[16]; Figure 1). DNA intercalation is the process by which compounds containing planar aromatic or heteroaromatic ring systems are inserted between the adjacent base pairs perpendicular to the axis of the DNA helix.^[17]

Intercalating agents share common structural features, which include planar polyaromatic system linked to a groove-binding side chain in addition to one or more cationic species^[15] (Figure 1). The presence of two groove-binding side chains, as in case of nogalamycin **5**, which contains two sugar moieties at both ends of its chromophore leads to a special type of interaction with DNA called threading intercalation, in which one sugar unit is oriented to the minor groove and the other to the major groove of DNA^[18] (Figure 2).

Quinoxaline nucleus is the backbone of many bioactive compounds,^[19–21] some of them have anticancer activities.^[22] The discovery and development of new therapeutic DNA intercalators for the treatment of cancer are considered one of the most important targets in the field of medicinal chemistry.^[23] Quinoxaline analogs exhibited excellent anticancer activities through DNA intercalation. For instance, echinomycin **6**, a natural DNA intercalator, showed potent activities in phase I and II trials against a wide array of cancer.^[24] Moreover, compound **7** was previously synthesized by our team and exhibited excellent Topo II inhibitory activity and DNA-binding affinity with the induction of apoptosis in Caco-2 cells.^[25]

On the basis of the earlier findings and in continuation of our previous efforts in the design and synthesis of new anticancer agents,^[26–29] especially Topo II inhibitors and DNA intercalators,^[25,30,31] we report the design, synthesis, DNA-binding, and docking studies of a new series of quinoxaline derivatives. These derivatives were designed based on the main pharmacophoric features of DNA intercalators.

1.1 | The rationale of the molecular design

A study of the structure–activity relationships (SAR) and binding pattern of DNA intercalators revealed that they shared three main features: (a) A planar polyaromatic system, which involves three or four fused rings (chromophore) binding with DNA. The chromophore is oriented with its long axis perpendicular to the long axis of the adjacent base pairs.^[32] Once the intercalator has been sandwiched between the DNA base pairs, the stability of the complex is optimized by a number of noncovalent interactions, including the van der Waals and π -stacking interactions.^[33] (b) Cationic species, which increase the efficiency of DNA intercalators by interaction with the negatively charged DNA sugar-phosphate backbone. The cationic species are basic groups (e.g., amino or nitrogen-containing heterocyclic groups) that can be protonated under physiological pH^[15] (Figure 1). (c) Groove-binding side chain, which can occupy the minor groove of DNA.^[34–36]

The rationale of our molecular design depended on the lead modification of our previously synthesized compound **7** through the generation of two scaffolds of [1,2,4]triazolo[4,3-*a*]quinoxaline derivatives. The scaffold **1** was 4-sulfanyl-[1,2,4]triazolo[4,3-*a*]quinoxaline moiety with a groove-binding side chain at position-4 (compounds **18a,b**, **19a–c**, **20**, **21**, **22**, and **23**) to act as classical DNA intercalators. The scaffold **2** was 1-sulfanyl-[1,2,4]triazolo[4,3-*a*]quinoxalin-4(5*H*)-one moiety with two groove-binding side chains at positions 1 and 4 (compounds **24a–g**, **25a–d**, **26**, **27**, and **28a,b**) to act as threading DNA intercalators. The choice of different substituents was based on their relatively high lipophilicity to pass the nuclear membranes aiming to have strong DNA intercalation.^[37] Moreover, the variability of substitutions enabled us to study the SAR of the final compounds (Figure 3).

In general, the synthesized compounds were evaluated for their *in vitro* antiproliferative activities against hepatocellular carcinoma (Hep G-2), human laryngeal carcinoma (Hep-2), and colorectal adenocarcinoma (Caco-2) cell lines. The results prompted further

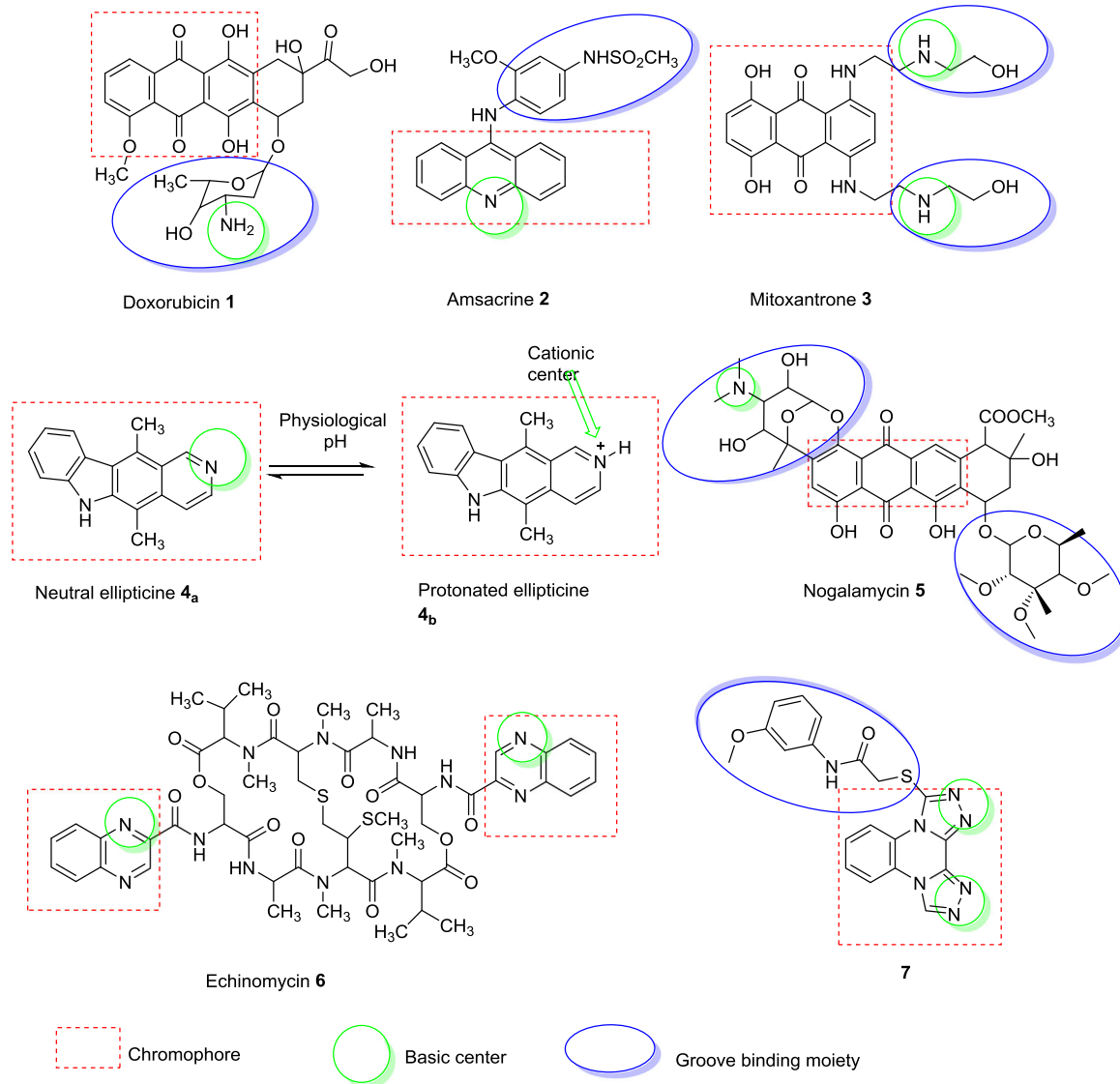


FIGURE 1 Some reported DNA intercalators and their basic pharmacophoric features

examinations to reach a deep insight into the mechanism of action. First, the most cytotoxic agents were further examined as potential Topo II inhibitors. Second, these compounds were evaluated to assess their binding affinities against DNA through DNA/methyl green assay. Third, the effect of the most active compound **19b** on apoptosis and cell cycle was investigated in Hep G-2 cell line. Fourth, gene expression analysis was done for compound **19b** in Hep G-2 cell line to determine the affected genes. Finally, molecular docking was carried out to examine the binding patterns with the prospective target, DNA-Topo II complex (PDB-code: 4G0U).

2 | RESULTS AND DISCUSSION

2.1 | Chemistry

For the synthesis of the title compounds, the sequence of the reactions is illustrated in Schemes 1–3. *o*-Phenylenediamine **8**

reacted with oxalic acid **9** in the presence of 4 N HCl to give 1,4-dihydroquinoxaline-2,3-dione **10**.^[38] The latter was treated with thionyl chloride to afford 2,3-dichloroquinoxaline **11**.^[38] Treatment of the 2,3-dichloroquinoxaline with hydrazine hydrate with continuous stirring at room temperature produced 2-chloro-3-hydrazinylquinoxaline **12**.^[39] Cyclization of **12** was carried out by heating with triethylorthoformate to give 4-chloro[1,2,4]triazolo[4,3-*a*]quinoxaline **13**.^[39] The reaction of **13** with thiourea in absolute alcohol with subsequent treatment with 10% KOH followed by acidification using conc. HCl produced [1,2,4]triazolo[4,3-*a*]quinoxaline-4-thiol **14**.^[40] Compound **15**,^[40] the potassium salt of **14**, was prepared by treatment of **14** with alc. KOH. ¹H NMR spectrum of **15** revealed the disappearance of exchangeable proton signals, in addition to the presence of a sharp singlet aromatic proton corresponding the methine group, which attached to two N-atoms; ¹³C and distortionless enhancement by polarization transfer (DEPT)-135 spectra of **15** showed an aromatic peak for the same group. On the contrary,

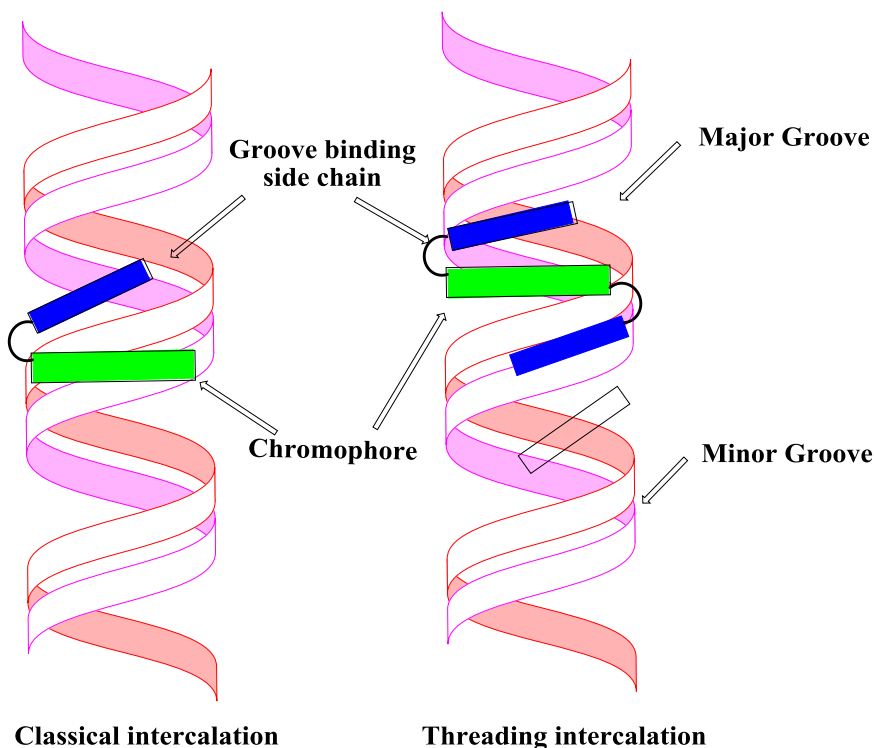


FIGURE 2 Schematic representation of the classical and threading DNA intercalation

compound **12** was allowed to react with CS_2 with the presence of KOH in absolute ethanol followed by acidification using diluted HCl (10%) to afford compound **16**. The dipotassium salt of 1-sulfanyl-[1,2,4]triazolo[4,3-a]quinoxalin-4(5H)-one **17** was prepared by heating compound **15** in alc. KOH solution (Scheme 1). The infrared (IR) spectrum of compound **16** demonstrated the stretching bands at 3,264, 2,550, and 1,693 cm^{-1} corresponding to NH, SH, and C=O, respectively.

The potassium salt **15** was treated with the appropriate 2-chloroacetamido or 3-chloropropanamido derivatives namely, 4-(2-chloroacetamido)benzoic acid and ethyl 4-(2-chloroacetamido)benzoate, 2-chloro-*N*-(4-sulfamoylphenyl)acetamide, 2-chloro-*N*-(4-(*N*-(pyridin-2-yl)sulfamoyl)phenyl) acetamide, and 2-chloro-*N*-(4-(*N*-(thiazol-2-yl)sulfamoyl)phenyl)acetamide, 3-chloro-*N*-(4-sulfamoylphenyl)propanamide, 3-chloro-*N*-(4-sulfamoylphenyl)propanamide, 2-chloroacetamide, and *N*-(4-acetylphenyl)-2-chloroacetamide in dry *N,N*-dimethylformamide (DMF) in the presence of KI as a catalyst to afford the corresponding compounds **18a,b**, **19a-c**, **20**, **21**, **22**, and **23**, respectively (Scheme 2). The IR spectra of these compounds demonstrated stretching bands at a range of 3,185–3,324 cm^{-1} corresponding to the NH amide groups, and other bands at a range of 1,672–1,691 cm^{-1} corresponding to C=O amide groups. In addition, the presence of NH_2 absorption bands at a range of 3180–3197 cm^{-1} for compounds **19a**, **20**, **21**, and **22**. ^1H NMR spectra of these compounds showed characteristic D_2O exchangeable signals at a range of 10.00–10.86 ppm corresponding to the NH amide groups, in addition to the presence of characteristic D_2O exchangeable signals at a range of 7.20–7.30 ppm corresponding to the NH_2 groups of compounds **19a**, **20**, **21**, and **22**. Moreover, ^1H NMR spectra showed singlet signals of aliphatic protons at a range of 4.13–4.45 ppm

corresponding to the SCH_2 protons. On the contrary, ^{13}C NMR and DEPT-135 spectra of **18a,b**, **19a-c**, **20**, **21**, **22**, and **23** show a characteristic peak for a deshielded methylene group corresponding to SCH_2 carbon. Also ^{13}C data reveals the presence of an ester and an amide carbonyl signals in the spectra of **18a** and **b** and the existence of an amide carbonyl signal in the spectra of **19a-c**, **20**, **21**, and **22**, whereas ^{13}C spectra of compound **23** showed the presence of a ketone and an amide carbonyl signals. All those carbonyl signals seems to have disappeared in the DEPT-135 spectra.

The dipotassium salt **17** was allowed to react with the different alkyl halids namely, methyl bromide, ethyl bromide, *n*-butyl bromide, *n*-hexyl, *n*-decyl bromide, allyl bromide, and benzyl bromide in dry DMF in the presence of KI as a catalyst to afford the corresponding target compounds **24a-g**, respectively. Moreover, compound **17** was further treated with the appropriate 2-chloroacetate or 2-chloropropanoate derivatives namely, methyl 2-chloroacetate, ethyl 2-chloroacetate, isopropyl 2-chloroacetate, and isobutyl 2-chloroacetate and methyl 2-chloropropanoate in dry DMF in the presence of KI as a catalyst to give the corresponding title compounds **25a-d**, **26**, respectively. The IR spectra of compounds **25a-d** and **26** demonstrated the stretching bands at 1,734 and 1,742 cm^{-1} corresponding to C=O groups of esters. Moreover, ^1H NMR of these compounds showed disappearance of the SH signal and appearance of aliphatic signal in the aliphatic region. Finally, the dipotassium salt **17** reacted with the appropriate 2-chloroacetamido derivatives namely, 4-(2-chloroacetamido)benzoic acid 2-chloro-*N*-(4-sulfamoylphenyl)acetamide and 2-chloro-*N*-(4-(*N*-(pyridin-2-yl)sulfamoyl)phenyl)acetamide in dry DMF to produce the corresponding final compounds **27** and **28a,b**, respectively (Scheme 3). The IR spectra of compounds **27** and **28a,b** demonstrated stretching bands

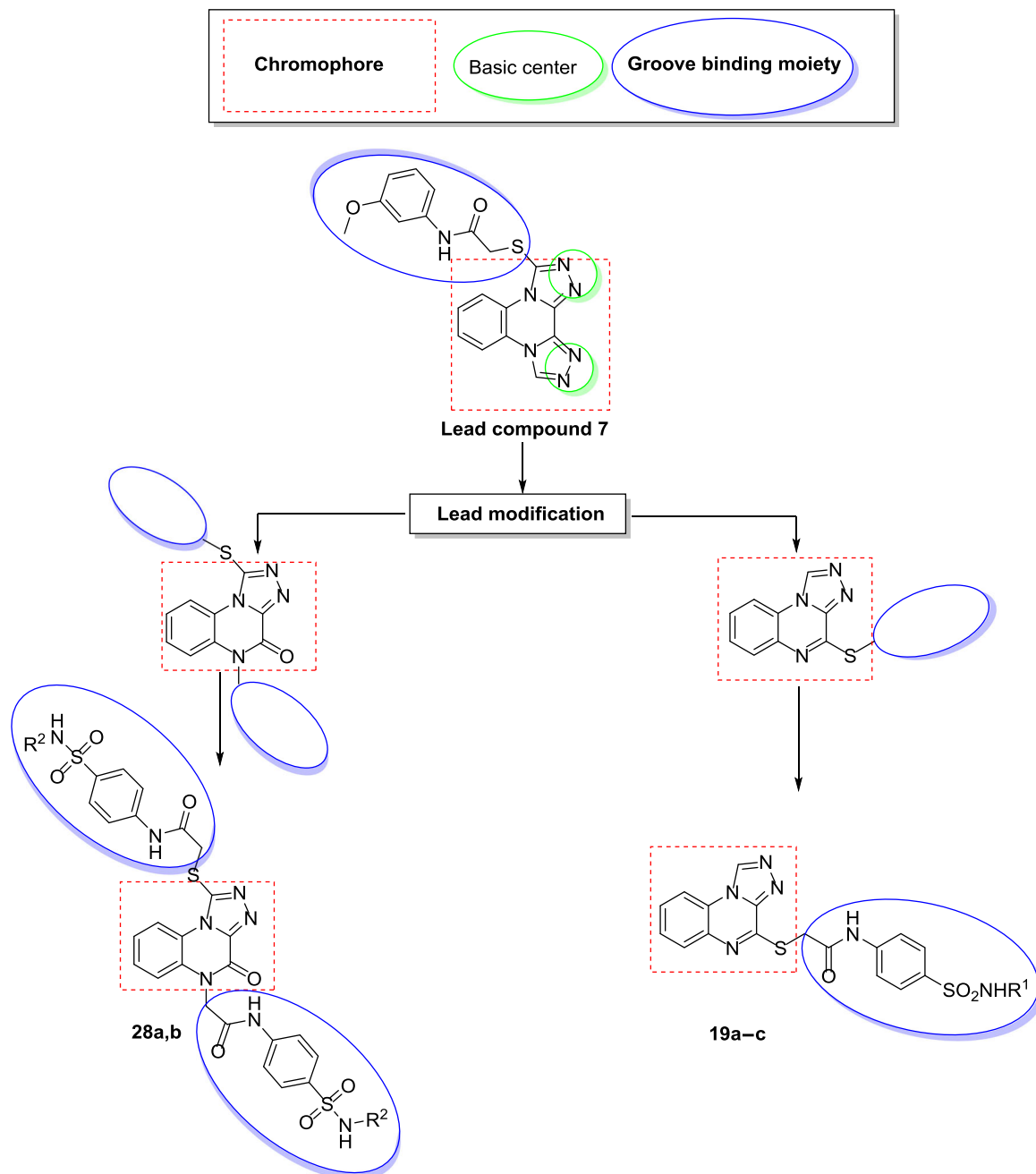


FIGURE 3 Rationale of the molecular design of new DNA intercalators

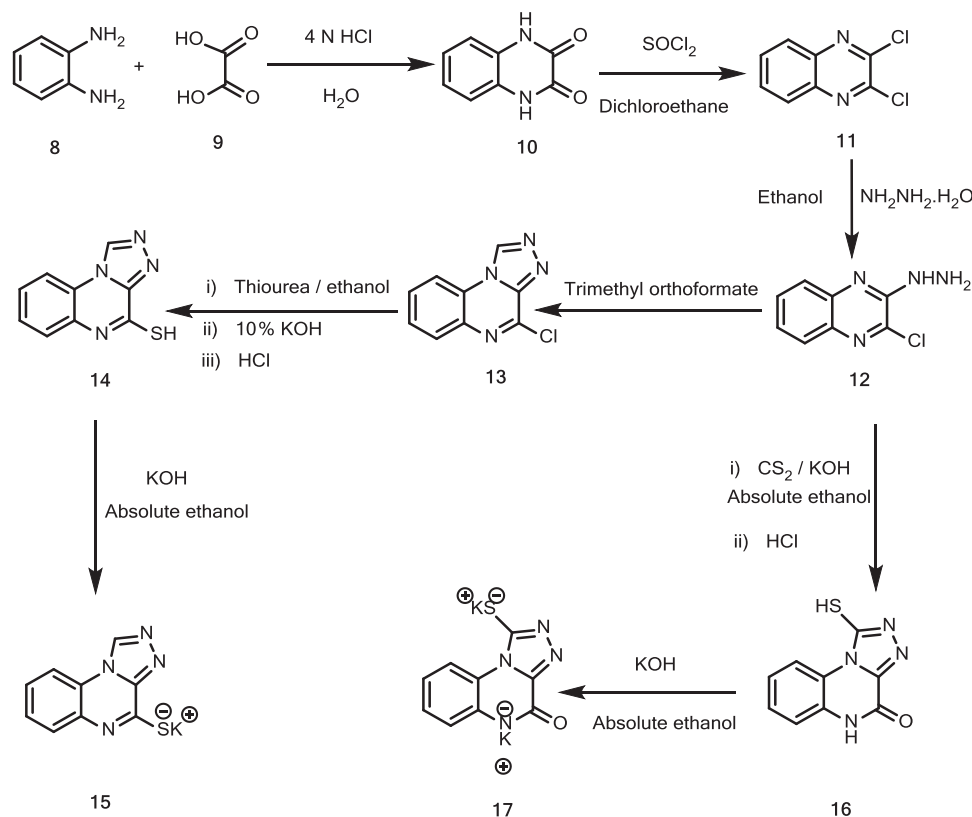
at 1,685, 1,675, and 1,687 cm^{-1} corresponding to the $\text{C}=\text{O}$ groups of these compounds, respectively. Moreover, ^1H NMR of these compounds showed exchangeable signals at a range of 10.53–10.98 ppm corresponding to the NH groups. The structures of all newly synthesized compounds were confirmed under the basis of spectral and elemental analyses, which were in full agreement with the proposed structures. On the contrary, ^{13}C NMR and DEPT-135 spectra of **24b–g**, **25a–d**, **27**, and **28a,b** show a characteristic peak for a deshielded methylene group corresponding to the SCH_2 carbon. Also, ^{13}C NMR and DEPT-135 spectra of **26** show a characteristic peak for a deshielded methine group corresponding to the SCH carbon. In addition, ^{13}C data reveals the presence of an amide

carbonyl signal in the spectra of **24a–g** and the existence of an amide and two ester carbonyl signals in the spectra of **25a–d** and **26**, whereas ^{13}C NMR spectra of compound **27** and **28a,b** showed the presence of three amide carbonyl signals. All those carbonyl signals seem to have disappeared in the DEPT-135 spectra.

2.2 | Biological evaluation

2.2.1 | In vitro antiproliferative activities

The synthesized compounds were tested for their antiproliferative activities against three different cancer cell lines: hepatocellular carcinoma (Hep G-2), human laryngeal carcinoma (Hep-2), and



SCHEME 1 General procedure for the preparation of target compounds 15–17

colorectal adenocarcinoma (Caco-2). Neutral red assay protocol was used in this test as described by Borenfreund and Puerner.^[41] Doxorubicin was used as a positive control. The IC₅₀ values of the synthesized compounds against the aforementioned cell lines are summarized in Table 1.

The results revealed that most of the synthesized compounds exhibited excellent, modest, or weak antiproliferative activities against the three cell lines. Overall, compounds **16**, **18b**, **19b**, **22**, **23**, **24a**, **25a**, **25b**, **26**, and **28b** showed excellent antiproliferative activities against all tested cancer cell lines with IC₅₀ values ranging from 0.26 to 5.26 μM.

In particular, compounds **18b**, **19b**, **23**, **25b**, and **26** were found to be the most potent members. Compound **18b** was 1.38, 0.47, and 0.36 times as active as doxorubicin against Hep G-2 (IC₅₀ = 0.55 ± 0.1 μM), Hep-2 (IC₅₀ = 1.37 ± 0.2 μM), and Caco-2 (IC₅₀ = 2.23 ± 0.1 μM), respectively. For compound **19b**, it was 1.52, 0.86, and 0.27 times as active as doxorubicin against Hep G-2 (IC₅₀ = 0.50 ± 0.1 μM), Hep-2 (IC₅₀ = 0.75 ± 0.1 μM), and Caco-2 (IC₅₀ = 2.91 ± 0.1 μM), respectively. Compound **23** was 2.37, 2.50, and 0.40 times as active as doxorubicin against Hep G-2 (IC₅₀ = 0.32 ± 0.1 μM), Hep-2 (IC₅₀ = 0.26 ± 0.1 μM), and Caco-2 (IC₅₀ = 1.99 ± 0.1 μM), respectively. Compound **25b** was 0.42, 0.58, and 0.57 times as active as doxorubicin against Hep G-2 (IC₅₀ = 1.79 ± 0.1 μM), Hep-2 (IC₅₀ = 1.11 ± 0.2 μM), and Caco-2 (IC₅₀ = 1.41 ± 0.1 μM), respectively. Compound **26** was 0.63, 0.31, and 1.35 times as active as doxorubicin against Hep G-2 (IC₅₀ = 1.19 ± 0.1 μM), Hep-2 (IC₅₀ = 2.08 ± 0.2 μM), and Caco-2 (IC₅₀ = 0.60 ± 0.1 μM), respectively.

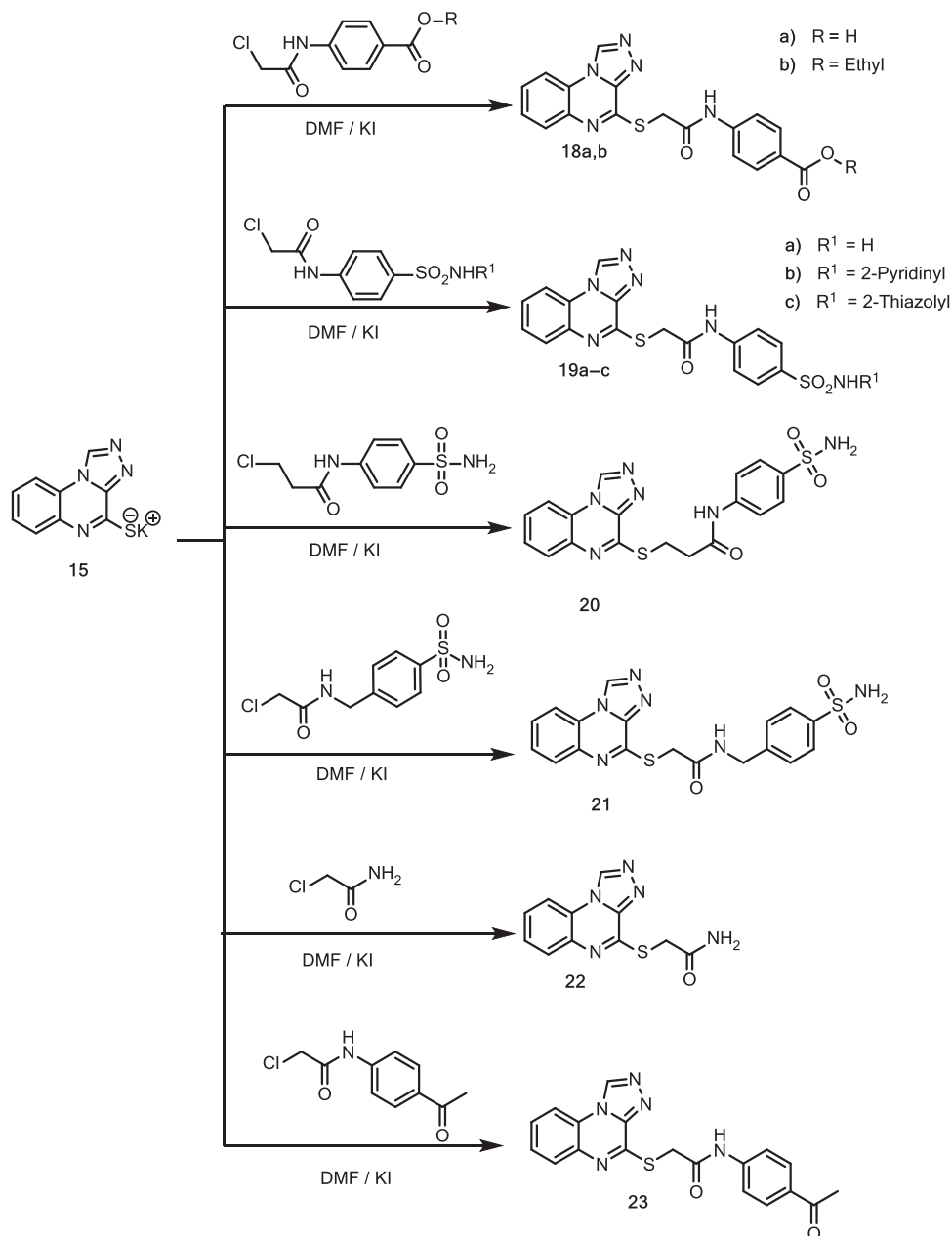
In addition, the compounds **19c**, **21**, **24b**, **24c**, **24f**, and **24g** showed superior antiproliferative activities against two tumor cell lines with IC₅₀ values ranging from 0.96 ± 0.1 to 4.79 ± 0.1 μM. Moreover, compounds **18a**, **19a**, **24e**, **25c**, **25d**, **27**, and **28a** were found to possess moderate antiproliferative activities toward at least two cell lines with IC₅₀ values ranging from 8.54 ± 0.2 to 18.39 ± 0.8 μM.

Finally, few compounds were found to possess weak antiproliferative activities against one or two cell lines with IC₅₀ values ranging from 26.63 ± 0.2 to 41.52 ± 0.2 μM.

2.2.2 | Topoisomerase II inhibitory activity

Twelve compounds showing the highest cytotoxic activities (**16**, **18b**, **19b**, **19c**, **22**, **23**, **24a**, **25a**, **25b**, **26**, **27**, and **28b**) were further examined as Topo II inhibitors, according to the reported method described by Furet et al.^[42] Doxorubicin was also tested using the same procedure as a positive control. The IC₅₀ values were calculated from the concentration–inhibition response curve and are summarized in Table 2.

As shown in Table 2, most of the tested compounds could interfere with the Topo II activity. They exhibited good to moderate inhibitory activities with IC₅₀ values ranging from 0.97 ± 0.1 to 5.07 ± 0.7 μM. To a great extent, the reported results were in agreement with the *in vitro* cytotoxicity activity. Among the active compounds, compound **19b** potently inhibited Topo II at a low IC₅₀ value (0.97 ± 0.1 μM). Also, compounds **16**, **19c**, **22**, **23**, **26**, **27**, and **28b** possessed low IC₅₀ values (1.57 ± 0.1, 1.10 ± 0.1, 1.68 ± 0.1, 1.12 ± 0.2, 1.72 ±



SCHEME 2 General procedure for the preparation of target compounds **18a,b**, **19a-c**, **20**, **21**, **22**, and **23**

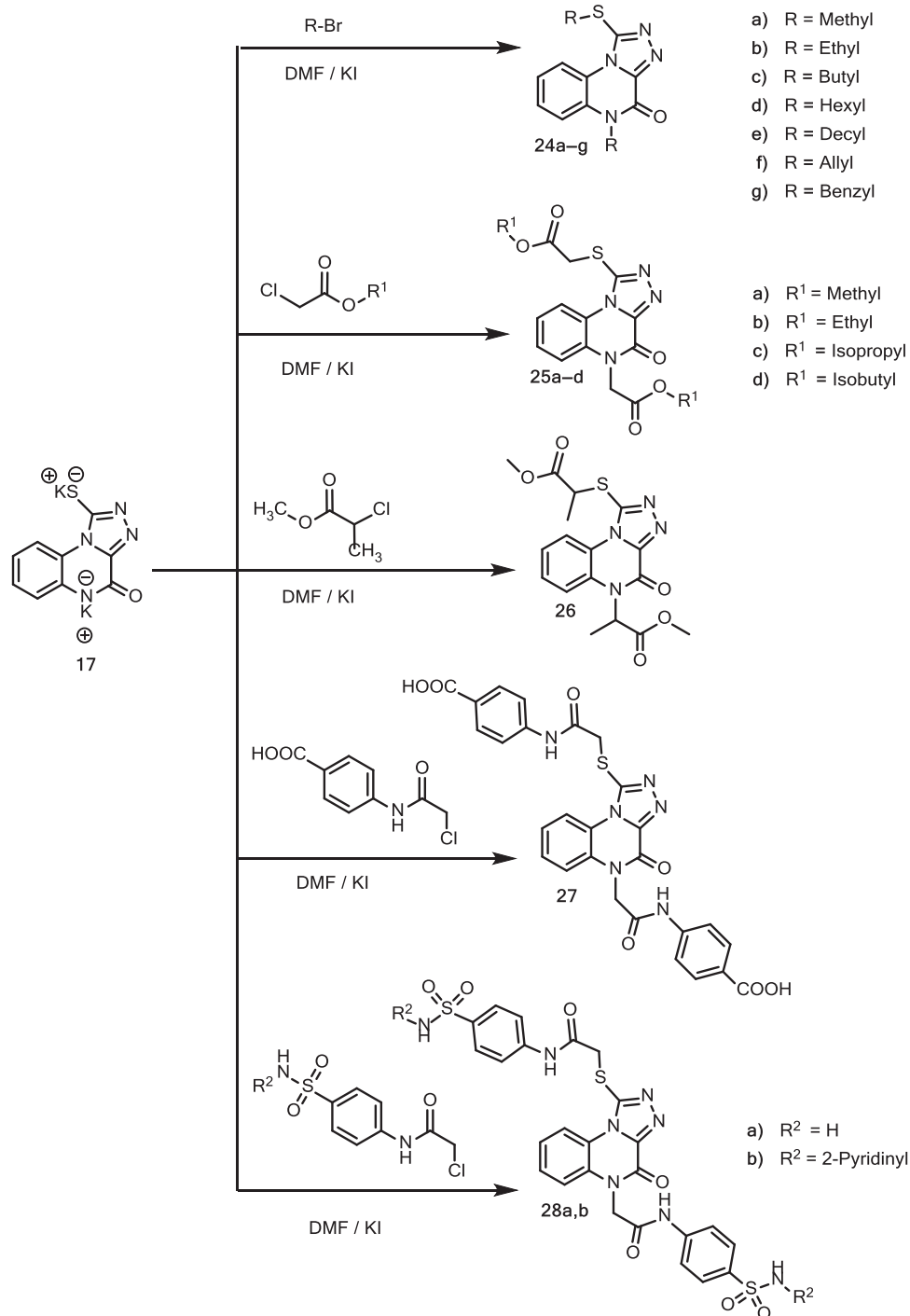
0.1, 1.70 ± 0.1 , and 1.62 ± 0.1 μM , respectively), compared with that of the reference drug, doxorubicin ($\text{IC}_{50} = 0.94 \pm 0.1$ μM). On the contrary, some compounds showed moderate activities, such as compounds **18b**, **24a**, **25a**, and **25b** ($\text{IC}_{50} = 2.89 \pm 0.2$, 3.06 ± 0.4 , 5.07 ± 0.7 , and 3.02 ± 0.2 μM , respectively).

2.2.3 | DNA intercalation assay (DNA/methyl green assay)

The most active antiproliferative derivatives (**16**, **18b**, **19b**, **19c**, **22**, **23**, **24a**, **25a**, **25b**, **26**, **27**, and **28b**) were selected

to evaluate their DNA-binding affinities using the methyl green dye according to the reported procedure described by Burres et al.^[43] The results of DNA-binding affinity are reported as IC_{50} values and summarized in Table 2. Doxorubicin, as one of the most powerful DNA intercalators, was used as a positive control.

The tested compounds displayed moderate DNA-binding affinities. Compound **28b** intercalated with DNA at an IC_{50} value of 37.06 ± 1.8 μM , while compounds **16**, **19b**, **19c**, **23**, **24a**, **26**, and **27** exhibited IC_{50} values of 50.19 ± 2.1 , 43.51 ± 2.0 , 49.11 ± 1.8 , 45.32 ± 2.2 , 53.93 ± 2.9 , 53.35 ± 3.4 , and 51.32 ± 1.9 μM , respectively. Finally, compounds **18b**,



SCHEME 3 General procedure for the preparation of target compounds **24a-g**, **25a-d**, **26**, **27**, and **28a,b**

22, **25a**, and **25b** showed higher IC_{50} values of 67.89 ± 4.1 , 77.62 ± 4.5 , 65.65 ± 3.9 , to 59.81 ± 3.7 μ M, respectively.

2.2.4 | Flow cytometric analysis of the cell cycle and apoptosis

Apoptosis or programmed cell death is a major control mechanism by which cells die if DNA damage exceeds the capacity of repair mechanisms. As part of normal development, apoptosis plays an

important role in controlling cell number and proliferation.^[44] Flow cytometric analysis is a rapid, reliable, and reproducible method that allows estimation and analysis of cell-cycle parameters of surviving cells.^[45] The most promising compound **19b** was further evaluated for its effect on the cell-cycle progression and induction of apoptosis in Hep G-2 cell lines. In this test, 0.5 μ M of compound **19b** was added to Hep G-2 cells with incubation for 24 hr, and the effect of such compound on the normal cell cycle and induction of apoptosis was analyzed.^[46]

TABLE 1 Antiproliferative activity of the synthesized compounds toward Hep G-2, Hep-2, and Caco-2 cell lines

Compound	IC ₅₀ (μM) ^a		
	Hep G-2	Hep-2	Caco-2
14	5.84 ± 0.5	32.81 ± 0.8	9.29 ± 0.9
16	0.64 ± 0.1	3.22 ± 0.1	2.88 ± 0.1
18a	1.58 ± 0.1	16.67 ± 0.9	8.54 ± 0.2
18b	0.55 ± 0.1	1.37 ± 0.2	2.23 ± 0.1
19a	3.91 ± 0.1	13.70 ± 0.9	15.25 ± 0.2
19b	0.50 ± 0.1	0.75 ± 0.1	2.91 ± 0.1
19c	0.96 ± 0.1	3.59 ± 0.3	10.13 ± 0.2
20	1.32 ± 0.2	41.52 ± 0.2	26.63 ± 0.2
21	1.03 ± 0.1	36.50 ± 0.9	1.05 ± 0.1
22	2.47 ± 0.1	5.69 ± 0.2	4.15 ± 0.1
23	0.32 ± 0.1	0.26 ± 0.1	1.99 ± 0.1
24a	0.90 ± 0.1	3.47 ± 0.2	5.26 ± 0.1
24b	1.05 ± 0.1	4.01 ± 0.2	38.52 ± 0.6
24c	1.31 ± 0.1	4.49 ± 0.1	32.56 ± 0.9
24d	1.67 ± 0.1	8.11 ± 0.6	29.92 ± 0.9
24e	9.11 ± 0.9	10.22 ± 0.1	16.89 ± 0.6
24f	2.52 ± 0.1	11.87 ± 0.4	4.79 ± 0.1
24g	1.12 ± 0.1	13.19 ± 0.2	3.07 ± 0.1
25a	3.87 ± 0.2	5.08 ± 0.1	3.05 ± 0.2
25b	1.79 ± 0.1	1.11 ± 0.2	1.41 ± 0.1
25c	16.86 ± 0.3	17.72 ± 0.9	15.46 ± 0.2
25d	10.13 ± 0.4	7.19 ± 0.1	8.34 ± 0.9
26	1.19 ± 0.1	2.08 ± 0.2	0.60 ± 0.1
27	2.34 ± 0.2	18.39 ± 0.8	9.52 ± 0.1
28a	4.09 ± 0.1	13.99 ± 0.7	18.20 ± 0.4
28b	2.87 ± 0.1	2.39 ± 0.1	3.27 ± 0.2
Doxorubicin	0.76 ± 0.1	0.65 ± 0.1	0.81 ± 0.1

Abbreviation: SD, standard deviation.

^aIC₅₀ values are the mean ± SD of three separate experiments.

The exposure of Hep G-2 cells to compound **19b** resulted in an interference with the normal cell-cycle distribution, where **19b** induced the accumulation of cells in G2/M phase by about threefolds (45.07%) and increased the percentage of cells in pre-G1 more than sevenfolds (14.18%) compared with the control values (16.31% and 2.04%, respectively). Such an increase was accompanied by a significant reduction in the percentage of cells at the G0-G1 (40.16%) and S phases (14.77%) of the cell cycle compared with the control (52.31% and 31.38%, respectively). The accumulation of cells in pre-G1 phase may have resulted from the degradation of the genetic materials, indicating a possible role of apoptosis, while the accumulation of the cells in G2/M phase may have resulted from the G2/M arrest (Table 3 and Figures 4 and 5). These findings revealed that apoptosis has a pivotal role in the cancer cell death induced by the synthesized compounds.

TABLE 2 In vitro enzymatic inhibitory activities of the most active compounds against Topo II and DNA intercalating affinity of the tested compounds

Compound	Topo II inhibition	DNA intercalation
	IC ₅₀ (μM) ^a	IC ₅₀ (μM) ^a
16	1.57 ± 0.1	50.19 ± 2.1
18b	2.89 ± 0.2	67.89 ± 4.1
19b	0.97 ± 0.1	43.51 ± 2.0
19c	1.10 ± 0.1	49.11 ± 1.8
22	1.68 ± 0.1	77.62 ± 4.5
23	1.12 ± 0.2	45.32 ± 2.2
24a	3.06 ± 0.4	53.93 ± 2.9
25a	5.07 ± 0.7	65.65 ± 3.9
25b	3.02 ± 0.2	59.81 ± 3.7
26	1.72 ± 0.1	53.35 ± 3.4
27	1.70 ± 0.1	51.32 ± 1.9
28b	1.62 ± 0.1	37.06 ± 1.8
Doxorubicin	0.94 ± 0.1	30.24 ± 1.2

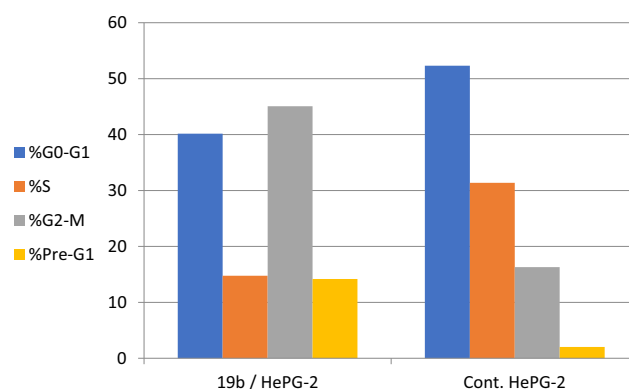
Abbreviation: SD, standard deviation.

^aIC₅₀ values are the mean ± SD of three separate experiments.**TABLE 3** Percentage of cell-cycle phases and pre-G1 apoptosis upon treatment with compound **19b** using Hep G-2 cells

Sample	G0-G1 (%)	S (%)	G2-M (%)	Pre-G1 (%)
19b/Hep G-2	40.16	14.77	45.07	14.18
Cont. Hep G-2 (negative control)	52.31	31.38	16.31	2.04

2.2.5 | Apoptosis induction

Annexin V/propidium iodide (PI) double-staining assay method was performed to investigate the mode of induced cell death in Hep G-2 cells at pre-G1 phase.^[47] Hep G-2 cells were treated with 0.5 μM of compound **19b** for 24 hr. In general, the total percentage of apoptosis induced by the treatment of Hep G-2 cells with compound **19b** was

**FIGURE 4** Schematic diagram for the percentage of Hep G-2 cells in each phase and the apoptosis effect upon treatment with 0.5 μM of compound **19b**

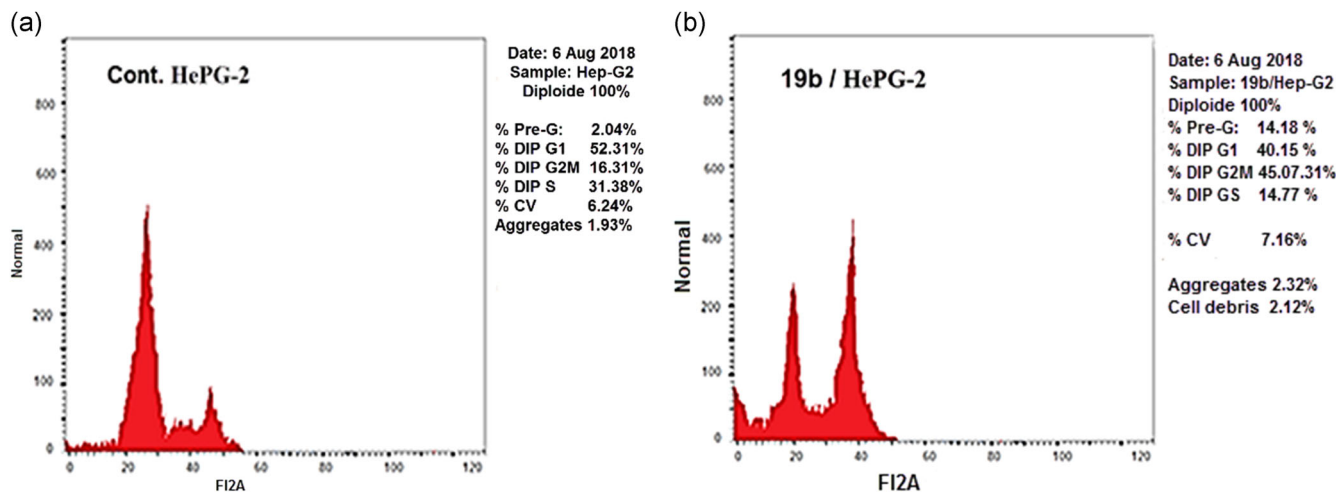


FIGURE 5 Cell-cycle analysis by flow cytometry: (a) control Hep G-2 cell line (negative control) and (b) the effect of compound **19b** on Hep G-2 cells

13.53. In the early stage, it was found that there is an increase in the percentage of apoptotic cells from 0.51% for control untreated cells to 4.25%, whereas in the late stage, there was an increase in the apoptotic cells from 0.25% for control Hep G-2 cells to 9.28%. From the obtained results, we can deduce that compound **19b** can induce pre-G1 apoptosis, as shown in Table 4 and Figures 6 and 7.

TABLE 4 Percent of cell death induced by compound **19b** on Hep G-2 cells

Sample	Apoptosis			
	Total	Early	Late	Necrosis
19b/Hep G-2	16.04	4.25	9.28	2.51
Cont. Hep G-2 (negative control)	2.04	0.51	0.25	1.28

2.2.6 | Gene expression analysis (RNA extraction and real-time RT-PCR for tested genes)

The gene expression pattern of compound **19b** was examined against the most sensitive cells (Hep G-2). The results can provide an additional insight into the possible molecular mechanisms of growth inhibition caused by the synthesized compounds. In this test, two of the most apoptosis-related factors (Bcl-2 and Bax genes) were determined. It was reported that Bcl-2 protein has an apoptosis resistance effect in hepatocellular carcinoma, moreover, Bcl-2 can inhibit apoptosis and promote the tumorigenesis and chemoresistance processes.^[48] On the contrary, the Bax gene can permit the triggering of the apoptotic pathway,^[49] and the drugs that activate Bax hold promise as anticancer agents by inducing apoptosis in cancer cells.^[50]

The results shown in Table 5 and Figure 8 revealed that the treatment of Hep G-2 cells with compounds **19b** reduced the

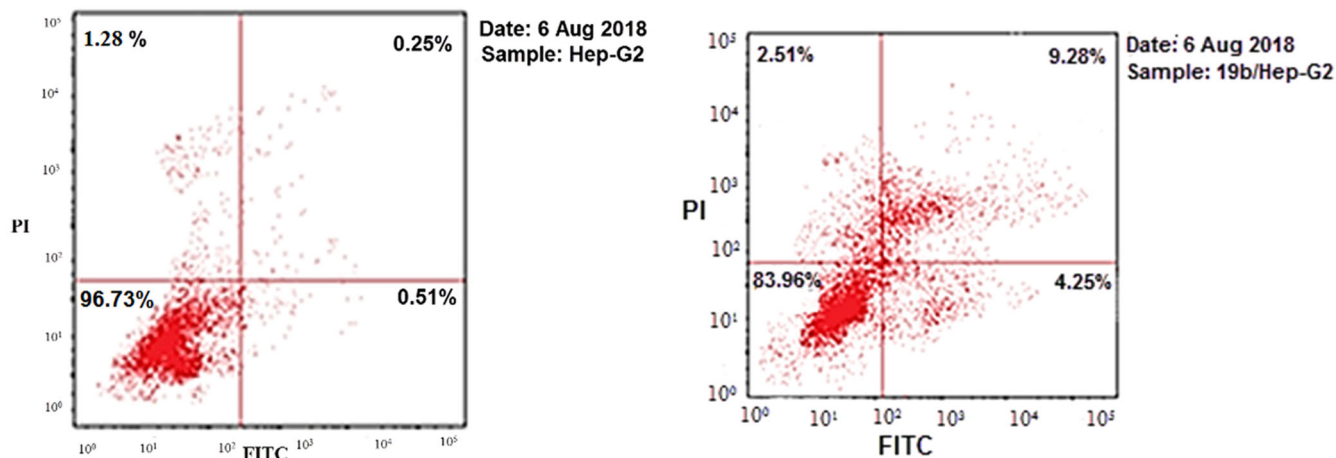


FIGURE 6 Flow cytometric assay with annexin V-FITC/PI double staining. Hep G-2 cells were treated with 0.5 μ M of compound **19b** for 24 hr, stained with annexin V-FITC and PI, and then measured by flow cytometer. FITC, fluorescein isothiocyanate; PI, propidium iodide

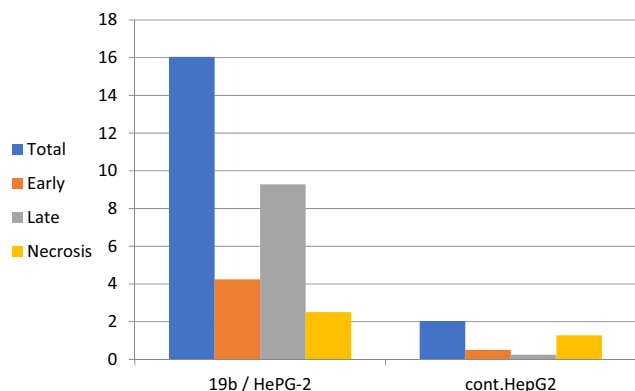


FIGURE 7 Schematic diagram for the percentage of cell death induced by compound **19b** on Hep G-2 cells

TABLE 5 RT-PCR in gene expression of Bcl-2 and Bax genes of Hep G-2 cells treated with compound **19b**

Gene	Control	Regulation ^a /19b	Effect
Bcl-2	332.82	117.52	Downregulated
Bax	947.51	472.19	Downregulated

^aThree independent experiments were performed.

expression levels of the anti-apoptotic protein Bcl-2 from 332.82 (control untreated cells) to 117.52. The ability of these compounds to downregulate Bcl-2 level, emphasizes its potential to enhance apoptosis. Also, it was found that compound **19b** downregulated the Bax gene.

2.3 | Molecular docking

2.3.1 | Docking studies

In this study, molecular docking investigational study was performed for the synthesized compounds and two reference DNA intercalators (doxorubicin and amsacrine). This study was carried out to gain further insight into the binding modes of the synthesized compounds

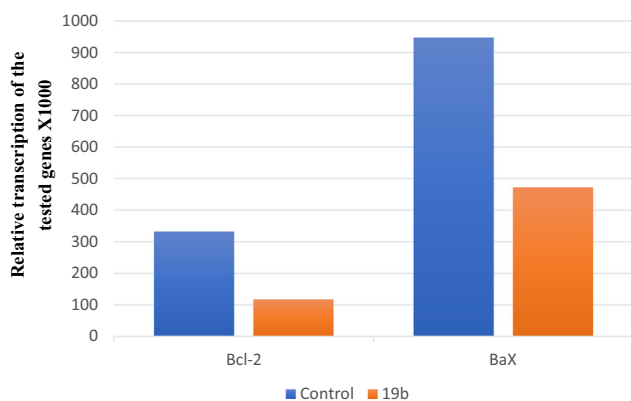


FIGURE 8 Schematic diagram for the real-time PCR data for Bax and Bcl-2 genes and their control

into the DNA-binding site of Topo II (PDB ID: 4G0U). The binding free energies (ΔG) are reported in Table 6. The negative values of free energies indicate the spontaneous nature of binding of the tested compound to the DNA-Topo II complex. The reported key binding site of DNA-Topo II consists of amino acid and nucleotide residues of Asp479, Arg503, Gln778, Met782 Cyt8, Thy9, Cyt11, Gua13, and Ade12.^[51]

The proposed binding mode of doxorubicin showed an affinity value equal to -82.10 kcal/mol. The planar aromatic system formed 13 aromatic stacking interactions with Ade12, Gua13, Cyt8, Thy9, and Ala521. It formed three hydrogen bonds with Gua13, Arg503, Lys505, and Lue502. The sugar moiety was oriented into the minor groove of DNA. These data were in agreement with the reported results^[52] (Figure 9).

The proposed binding mode of amsacrine showed affinity value equal to -55.56 kcal/mol and a root-mean-square deviation value of 1.01. The planar aromatic system formed 14 aromatic stacking interactions with Ade12, Gua13, Cyt8, and Thy9. The methoxy group formed a hydrogen bond with Gua13. The NH group formed a hydrogen bond with Glu522. *N*-(3-Methoxyphenyl)methanesulfonamide side-chain provided secondary interactions with the DNA minor groove (Figure 10).

The obtained results indicated that most of the studied ligands have similar position and orientation inside the putative binding site of doxorubicin and amsacrine. The designed molecules showed binding energies ranging from -34.44 to -65.47 kcal/mol (Table 6).

The proposed binding mode of compound **19b** showed an affinity value of -50.01 kcal/mol. It exhibited a mode of classical intercalation with DNA. It showed one hydrogen bond interaction between the NH group of acetamide moiety and Glu522. In addition, the planar aromatic system ([1,2,4]triazolo[4,3-*a*]quinoxaline) formed 14 aromatic stacking interactions with Ade12, Gua13, Cyt8, and Thy9.

TABLE 6 The calculated ΔG (binding free energies) of the synthesized compounds and reference drugs against DNA-topoisomerase II complex

Compound	ΔG (kcal/mol)	Compound	ΔG (kcal/mol)
14	-47.57	24d	-40.30
16	-48.31	24e	-50.33
18a	-55.49	24f	-35.40
18b	-51.62	24g	-45.11
19a	-48.68	25a	-47.45
19b	-50.01	25b	-50.98
19c	-51.44	25c	-51.00
20	-50.82	25d	-52.12
21	-48.38	26	-46.15
22	-38.04	27	-63.13
23	-55.00	28a	-65.47
24a	-34.44	28b	-60.01
24b	-37.01	Doxorubicin	-82.10
24c	-37.88	Amsacrine	-55.56

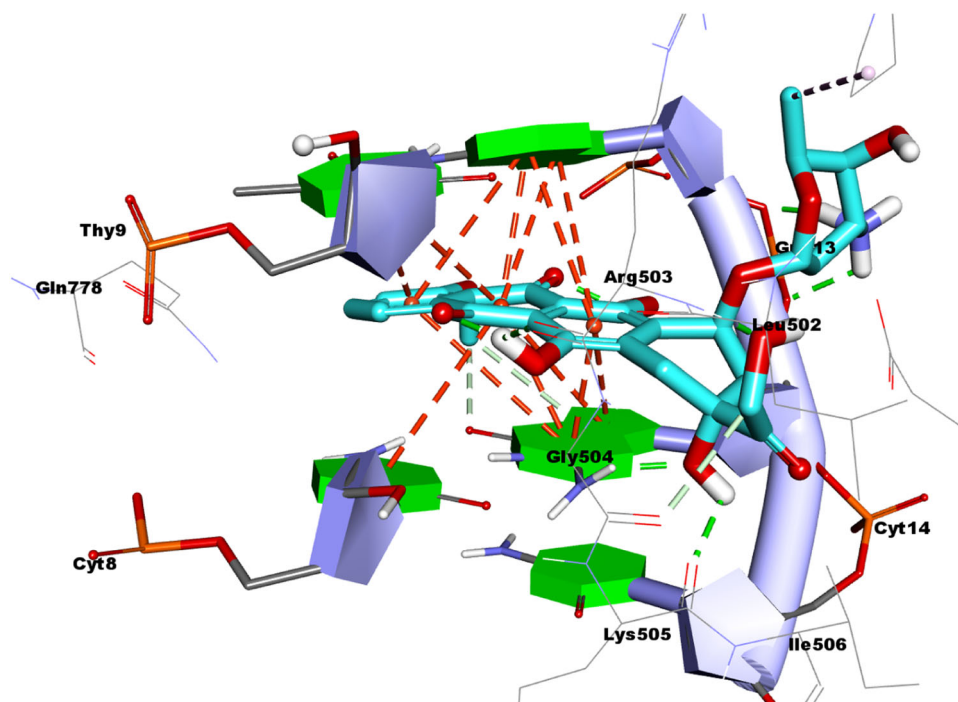


FIGURE 9 Binding of doxorubicin with Topo II. The hydrogen bonds are represented in green dashed lines and the π interactions are represented in orange dashed lines

Moreover, the terminal *N*-(4-(*N*-(pyridin-2-yl)sulfamoyl)phenyl)acetamide moiety was oriented at the minor groove of DNA, forming two hydrophobic interactions with Ala521 (Figure 11).

Compound **27** showed an affinity value of -63.13 kcal/mol. It exhibited a mode of threading intercalation with DNA, where one 4-acetamidobenzoic side chain was oriented at the minor groove of DNA, forming one hydrogen bond with Arg503 and two

hydrophobic interactions with Ala521 and Pro544. The other 4-acetamidobenzoic side chain was oriented at the major groove, forming four hydrogen bonds with Gua5, Gua7, and Gua13. Also, it formed one hydrophobic interaction with Met782. Moreover, the planar aromatic system ([1,2,4]triazolo[4,3-*a*]quinoxalin-4(5*H*)-one) formed sixteen aromatic stacking interactions with Ade12, Gua13, Cyt8, and Thy9 (Figure 12).

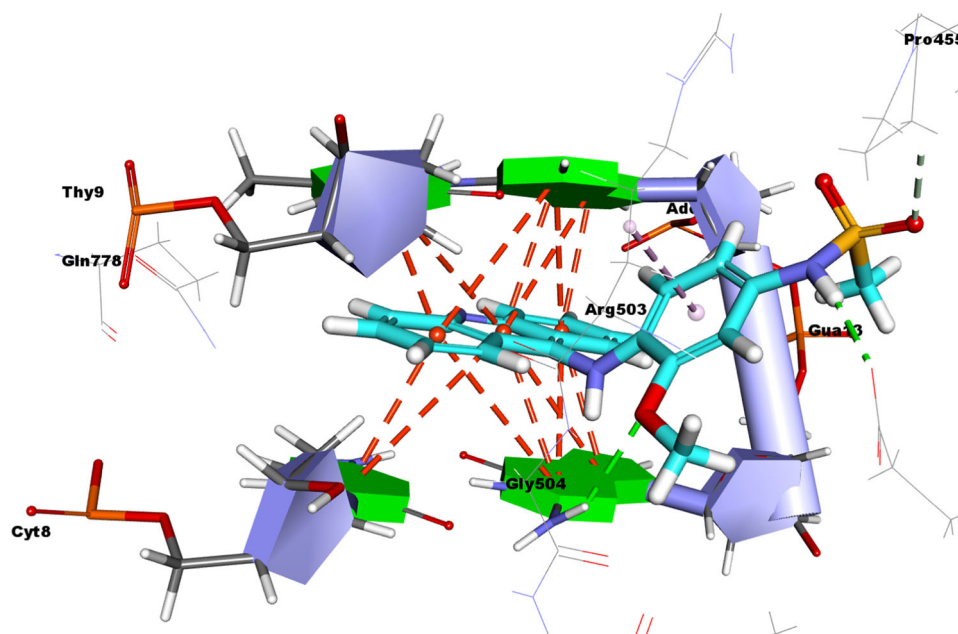


FIGURE 10 Binding of amsacrine with Topo II. The hydrogen bonds are represented in green dashed lines and the π interactions are represented in orange dashed lines

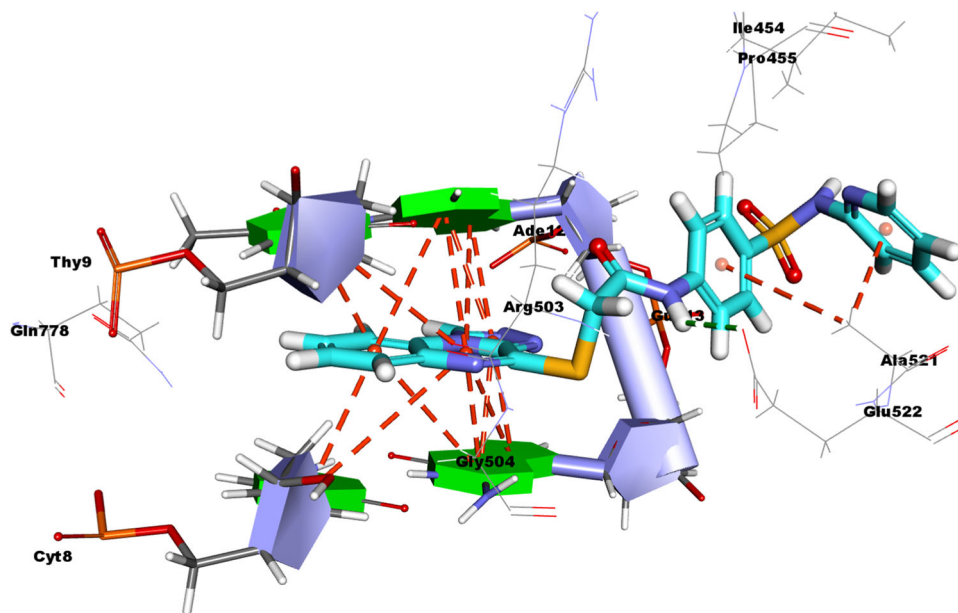


FIGURE 11 Binding of compound **19b** with Topo II. The hydrogen bonds are represented in green dashed lines and the π interactions are represented in orange dashed lines

2.4 | Structure–activity relationship (SAR)

In general, structure–activity correlation of the synthesized compounds against Hep G-2, Hep-2 and Caco-2 cell lines revealed that the unsubstituted 1-sulfanyl-[1,2,4]triazolo[4,3-*a*]quinoxalin-4(5*H*)-one (scaffold 2) **16** was more active than the unsubstituted 4-sulfanyl-[1,2,4]triazolo[4,3-*a*]quinoxaline (scaffold 1) **14**. On the contrary, the substituted 4-sulfanyl-[1,2,4]triazolo[4,3-*a*]quinoxaline derivatives (scaffold 1) were more active than the substituted 1-sulfanyl-[1,2,4]triazolo[4,3-*a*]quinoxalin-4(5*H*)-one derivatives (scaffold 2). These findings became clear by comparing the cytotoxicity of

the two scaffolds having the same substituents with each other. For example, compound **18a** (4-acetamidobenzoic acid derivative) incorporating scaffold 1 has decreased IC_{50} values against Hep G-2, Hep-2, and Caco-2 cell lines (1.58 ± 0.1 , 16.67 ± 0.9 , and 8.54 ± 0.2 μ M, respectively) compared with the corresponding member **27** incorporating scaffold 2 (2.34 ± 0.2 , 18.39 ± 0.8 , and 9.52 ± 0.1 μ M, respectively). Also, compound **19a** (*N*-(4-sulfamoyl-phenyl)acetamide derivative) incorporating scaffold 1 has decreased the IC_{50} values against Hep G-2, Hep-2, and Caco-2 cell lines (3.91 ± 0.1 , 13.70 ± 0.9 , and 15.25 ± 0.2 μ M, respectively) than the

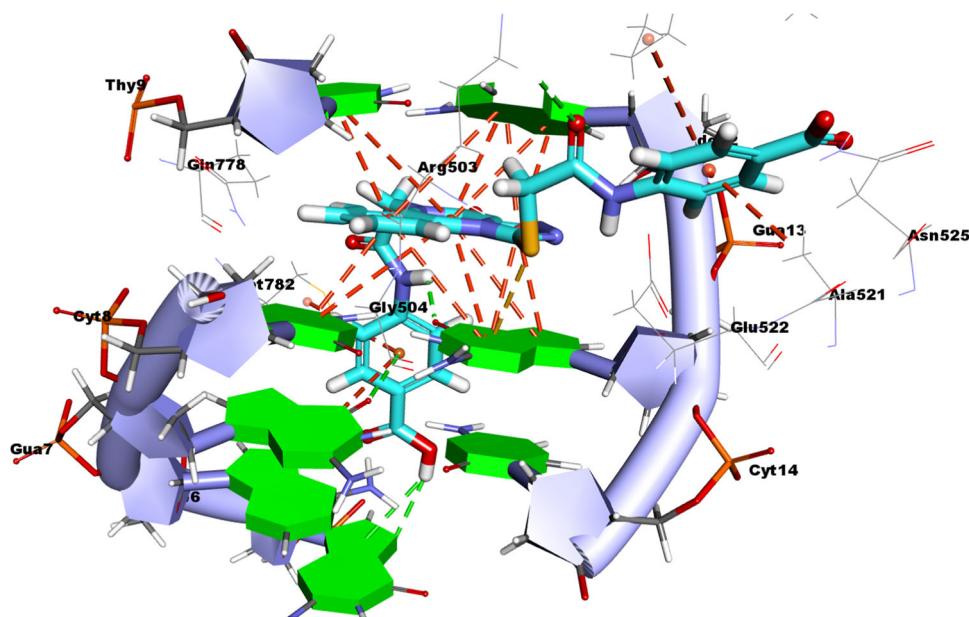


FIGURE 12 Binding of compound **27** with Topo II. The hydrogen bonds are represented in green dashed lines and the π interactions are represented in orange dashed lines

corresponding member **28a** incorporating scaffold 2 (4.09 ± 0.1 , 13.99 ± 0.7 , and $18.20 \pm 0.4 \mu\text{M}$). In addition, compound **19b** (*N*-(4-(*N*-pyridin-2-yl)sulfamoyl)phenyl)acetamide derivative) incorporating scaffold 1 has lower IC_{50} values against Hep G-2, Hep-2, and Caco-2 cell lines (0.50 ± 0.1 , 0.75 ± 0.1 , and $2.91 \pm 0.1 \mu\text{M}$, respectively) than the corresponding member **28b** incorporating scaffold 2 (2.87 ± 0.1 , 2.39 ± 0.7 , and $3.27 \pm 0.2 \mu\text{M}$, respectively).

Then, we explored the effect of substitution on the thiol group of 4-sulfanyl-[1,2,4]triazolo[4,3-*a*]quinoxaline nucleus (scaffold 1) by different moieties. It was found that compound **23** incorporating *N*-(4-acetylphenyl)acetamide moiety ($\text{IC}_{50} = 0.32 \pm 0.1$, 0.26 ± 0.1 , and $1.99 \pm 0.1 \mu\text{M}$) had higher activity than the corresponding members incorporating other moieties. With regard to the effect of other moieties, the activities decreased in the order of *N*-(4-sulfamoylphenyl)acetamide derivative **19b** > 4-acetamidobenzoic acid derivatives **18b** > *N*-(4-sulfamoylbenzyl)acetamide derivative **21** > *N*-(4-sulfamoylphenyl)propionamide derivative **20** > acetamide derivative **22**. Moreover, it was found that ethyl benzoate derivative **18b** was more active than free benzoic acid derivative **18a**. In addition, *N*-(pyridin-2-yl)benzenesulfonamide derivative **19b** showed better activity than the *N*-(thiazol-2-yl)benzenesulfonamide derivative **19c**, and the latter exhibited higher activity than free benzenesulfonamide derivative **19a**.

Next, we explored the impact of substitution on 1-sulfanyl-[1,2,4]triazolo[4,3-*a*]quinoxalin-4(5*H*)-one nucleus (scaffold 2) by different moieties. It was found that the activities decreased in the order of methyl propionate derivative **26** > alkyl derivatives **24a-g** > alkyl acetate derivatives **25a-d** > *N*-(4-sulfamoylphenyl)acetamide derivatives **28a,b** > 4-acetamidobenzoic acid derivative **27**. Concerning the activities of derivatives with alkyl substitutions **24a-g**, it was found that increasing lengths of alkyl chain led to decreased cytotoxic activities (methyl **24a** > ethyl **24b** > butyl **24c** > hexyl **24d** > decyl **24e**). With regard to the effect of substitution with alkyl acetates **25a-d**, it was found that activities decreased in the order of ethyl acetate **25b** > methyl acetate **25a** > isobutyl acetate **25d** > isopropyl acetate **25c**. Finally, it was found that *N*-(pyridin-2-yl)benzenesulfonamide derivative **28b** showed better activity than free benzenesulfonamide derivative **28a**.

3 | CONCLUSION

In summary, 26 derivatives of 4-sulfanyl-[1,2,4]triazolo[4,3-*a*]quinoxaline (scaffold 1) and 1-sulfanyl-[1,2,4]triazolo[4,3-*a*]quinoxalin-4(5*H*)-one (scaffold 2) have been designed and synthesized. Some compounds showed potent antiproliferative activities against Hep G-2, Hep-2, and Caco-2 cancer cell lines such as **18b** ($\text{IC}_{50} = 0.55 \pm 0.1$, 1.37 ± 0.2 , and $2.23 \pm 0.1 \mu\text{M}$, respectively), **19b** ($\text{IC}_{50} = 0.50 \pm 0.1$, 0.75 ± 0.1 , and $2.91 \pm 0.1 \mu\text{M}$, respectively), **23** ($\text{IC}_{50} = 0.32 \pm 0.1$, 0.26 ± 0.1 , and $1.99 \pm 0.1 \mu\text{M}$, respectively), **25b** ($\text{IC}_{50} = 1.79 \pm 0.1$, 1.11 ± 0.2 , and $1.41 \pm 0.1 \mu\text{M}$, respectively), and **26** ($\text{IC}_{50} = 1.19 \pm 0.1$, 2.08 ± 0.2 , and $0.60 \pm 0.1 \mu\text{M}$, respectively). Moreover, some compounds displayed potent inhibitory activities against Topo II as

compound **19b** ($\text{IC}_{50} = 0.97 \pm 0.1 \mu\text{M}$). DNA intercalation assay revealed that some of the synthesized compounds moderately bind to DNA such as compound **28b** ($\text{IC}_{50} = 37.06 \pm 1.8 \mu\text{M}$). In addition, flow cytometry analysis demonstrated that **19b** could significantly induce apoptosis (13.53%) of Hep G-2 cell at a concentration of 0.5 μM and can arrest the cell cycle at the G2/M phase. The SAR study revealed that substituted scaffold 1 showed better activity than the substituted scaffold 2. These results indicate that derivatives of the two scaffolds can act as potent Topo II inhibitors and effective anticancer agents. In addition, optimization of these derivatives may result in discovering more promising Topo II inhibitors.

4 | EXPERIMENTAL

4.1 | Chemistry

4.1.1 | General

All melting points (m.p.) were carried out by an open capillary method on a Gallenkamp melting point apparatus and were uncorrected. The IR spectra were carried out on a Pye-Unicam SP-3-300 infrared spectrophotometer (KBr disks) and expressed in wavenumber (cm^{-1}). ^1H NMR spectra were recorded at 400 MHz, on Bruker BioSpin GmbH 400 and 500 NMR spectrometers (Bruker, Rheinstetten, Germany), whereas ^{13}C NMR spectra were run at 100 MHz. TMS was used as an internal standard in deuterated dimethylsulfoxide ($\text{DMSO}-d_6$). Chemical shifts (δ) are quoted in ppm. The abbreviations used are as follows: s, singlet; d, doublet; m, multiplet. All coupling constant (*J*) values were given in Hertz. The mass spectra were recorded on Shimadzu GCMS-QP-1000EX mass spectrometer at 70 eV. Elemental analyses were performed on a CHN analyzer and all compounds were within ± 0.4 of the theoretical values. The reactions were monitored by thin-layer chromatography (TLC) using TLC sheets coated with UV fluorescent silica gel Merck 60 F_{254} plates and were visualized using UV lamp and different solvents as mobile phases. Compounds **10**, **11**, **12**, **13**, **14**, and **15** were synthesized according to the reported methods.^[38-40]

The InChI codes of the investigated compounds together with some biological activity data are provided as Supporting Information.

4.1.2 | Synthesis of sulfanyl-[1,2,4]triazolo[4,3-*a*]quinoxalin-4(5*H*)-one (**16**)

A mixture of 2-chloro-3-hydrazinylquinoxaline **12** (1.94 g, 0.01 mol), carbon disulfide (0.76 g, 0.71 ml, 0.03 mol), and potassium hydroxide (0.56 g, 0.02 mol) was refluxed in absolute ethanol (30 ml) for 4 hr. Then, the reaction mixture was concentrated, cooled to room temperature, and acidified with diluted hydrochloric acid. The obtained precipitate was filtered, washed with water, and recrystallized from ethanol to give compound **16**.

Yellow crystals (yield, 65%); m.p. = 180–182°C. IR (KBr, cm^{-1}): 3,073 (CH aromatic), 2,935 (CH aliphatic), 1,693 (C=O), and 1,597 (C=N); ^1H NMR ($\text{DMSO}-d_6$) δ (ppm): 7.34–7.38 (dd, 1H, *J* = 7.2, 8.8

Hz, Ar-H, H-8 of quinoxaline), 7.44–7.48 (dd, 1H, $J = 7.2, 8.4$ Hz, Ar-H, H-7 of quinoxaline), 7.51–7.54 (d, 1H, $J = 8.4$ Hz, Ar-H, H-6 of quinoxaline), 10.15 (d, 1H, $J = 8.8$ Hz, Ar-H, H-9 of quinoxaline), 13.74 (s, 1H, NH, D₂O exchangeable), 14.55 (s, 1H, SH, D₂O exchangeable); ¹³C NMR (DMSO-*d*₆, 100 MHz) δ (ppm): 121.16, 121.86, 129.28, 130.17, 132.85, 133.80, 149.36, 169.00, and 176.87; DEPT (DMSO-*d*₆, 100 MHz) δ (ppm): 121.16, 121.86, 129.28, and 132.85 (4CH); Anal. calcd. for C₉H₆N₄OS (218.23): C, 49.53; H, 2.77; N, 25.67. Found: C, 49.22%; H, 2.48%; N, 25.31%.

4.1.3 | Potassium 4-oxo-1-sulfido-4H-[1,2,4]triazolo-[4,3-*a*]quinoxalin-5-ide (17)

A mixture of **16** (2.18 g, 0.01 mol) and potassium hydroxide (1.12 g, 0.02 mol) in absolute ethanol (20 ml) was refluxed for 0.5 hr. Upon cooling to room temperature, a yellow precipitate was obtained, which was collected and washed with diethyl ether to afford the corresponding potassium salt **17**. Yield, 97%; m.p.: >300°C. Anal. calcd. for C₉H₄K₂N₄OS (294.41); Calcd.: C, 36.72; H, 1.37; N, 19.03. Found: C, 36.40%; H, 1.66%; N, 19.45%.

4.1.4 | General procedure for the synthesis of compounds **18a,b**, **19a–c**, **20**, **21**, **22**, **23**

A mixture of the potassium salt **15** (2.40 g, 0.01 mol) and the appropriate 2-chloro-acetamido or 3-chloropropanamido derivatives (0.01 mol) namely, 4-(2-chloroacetamido)benzoic acid and ethyl 4-(2-chloroacetamido)benzoate, 2-chloro-*N*-(4-sulfamoyl-phenyl)acetamide, 2-chloro-*N*-(4-(*N*-(pyridin-2-yl)sulfamoyl)phenyl)acetamide, and 2-chloro-*N*-(4-(*N*-(thiazol-2-yl)sulfamoyl)phenyl)acetamide, 3-chloro-*N*-(4-sulfamoyl-phenyl)propanamide, 3-chloro-*N*-(4-sulfamoyl-phenyl)propanamide, 2-chloroacetamide and *N*-(4-acetylphenyl)-2-chloroacetamide in dry DMF (30 ml) was heated on a water bath for 3 hr. After cooling, the reaction mixture was poured onto ice water (250 ml) with continuous stirring. The formed precipitate was filtered, washed with water, dried, and crystallized from methanol to afford the corresponding compounds **18a,b**, **19a–c**, **20**, **21**, **22**, and **23**, respectively.

4-(2-[[1,2,4]Triazolo[4,3-*a*]quinoxalin-4-ylthio]acetamido)benzoic acid (**18a**)

Buff crystals (yield, 60%); m.p. = 270–271°C. IR (KBr, cm⁻¹): 3,516 (OH), 3,248 (NH), 3,079 (CH aromatic), 2,925 (CH aliphatic), 1,692 and 1,673 (2C=O), and 1,596 (C=N); ¹H NMR (DMSO-*d*₆) δ (ppm): 4.42 (s, 2H, CH₂), 7.53 (dd, 1H, $J = 7.5, 8.0$ Hz, Ar-H, H-8 of quinoxaline), 7.59 (dd, 1H, $J = 7.5, 8.4$ Hz, Ar-H, H-7 of quinoxaline), 7.74 (d, 1H, $J = 8.0$ Hz, Ar-H, H-9 of quinoxaline), 7.77 (d, 1H, $J = 8.4$ Hz, Ar-H, H-6 of quinoxaline), 7.91 (d, 2H, $J = 7.6$ Hz, Ar-H, H-3, and H-5 of phenyl), 8.25 (d, 2H, $J = 7.6$ Hz, Ar-H, H-2, and H-6 of phenyl), 10.05 (s, 1H, Ar-H, N-CH=N), 10.81 (s, 1H, exchangeable with D₂O, -NH), 12.74 (s, 1H, exchangeable with D₂O, -OH); ¹³C NMR (DMSO-*d*₆, 100 MHz) δ (ppm): 34.52, 116.98, 118.89(2), 123.92, 126.22, 128.22, 128.59, 130.91(2), 135.48, 138.18,

141.76, 141.88, 143.31, 151.53, 166.86, and 167.55; DEPT (DMSO-*d*₆, 100 MHz) δ (ppm): 34.53 (1CH₂), 116.97, 118.88(2), 128.22, 128.59, 130.91(2), 138.18. 167.55 (9CH); MS (*m/z*): 379 (M⁺, 10.9%), 334 (41.9%), and 169 (100% base peak); Anal. calcd. for C₁₈H₁₃N₅O₃S (379.39): C, 56.99; H, 3.45; N, 18.46. Found: C, 56.52%; H, 3.71%; N, 18.82%.

Ethyl 4-(2-[[1,2,4]triazolo[4,3-*a*]quinoxalin-4-ylthio]acetamido)benzoate (**18b**)

Yellow crystals (yield, 65%); m.p. = 218–220°C. IR (KBr, cm⁻¹): 3,256 (NH), 3,082 (CH aromatic), 2,983 (CH aliphatic), 1,712, and 1,672 (2C=O), and 1,603 (C=N); ¹H NMR (DMSO-*d*₆) δ (ppm): 1.30 (t, 3H, $J = 7.0$ Hz, CH₃), 4.29 (q, 2H, OCH₂, $J = 7.0$ Hz), 4.42 (s, 2H, SCH₂), 7.61 (dd, 1H, $J = 7.5, 8$ Hz, Ar-H, H-8 of quinoxaline), 7.65 (dd, 1H, $J = 7.5, 8$ Hz, Ar-H, H-7 of quinoxaline), 7.77 (d, 2H, $J = 8.5$ Hz, Ar-H, H-3, and H-5 of phenyl), 7.85 (d, 1H, $J = 8$ Hz, Ar-H, H-9 of quinoxaline), 7.92 (d, 2H, $J = 8.5$ Hz, Ar-H, H-2, and H-6 of phenyl), 8.31 (d, 1H, $J = 7.5$ Hz, Ar-H, H-6 of quinoxaline), 10.04 (s, 1H, Ar-H, N-CH=N), 10.68 (s, 1H, exchangeable with D₂O, -NH); ¹³C NMR (DMSO-*d*₆, 100 MHz) δ (ppm): 14.62, 34.47, 60.84, 117.02, 119.11(2), 124.02, 125.10, 128.24, 128.33, 128.66, 130.66(2), 135.59, 138.14, 141.86, 143.67, 151.58, 165.78, and 168.91; DEPT (DMSO-*d*₆, 100 MHz) δ (ppm): 14.62, 34.47, 60.84, 117.02, 119.11(2), 128.24, 128.33, 128.66, 130.66(2), and 138.14; MS (*m/z*): 407 (M⁺, 9.08%), 170 (9.94%), 119 (66.91%), and 64.98 (100% base peak); Anal. calcd. for C₂₀H₁₇N₅O₃S (407.11): C, 58.96; H, 4.21; N, 17.19. Found: C, 58.57%; H, 3.81%; N, 17.52%.

2-[[1,2,4]Triazolo[4,3-*a*]quinoxalin-4-ylthio]-*N*-(4-sulfamoylphenyl)acetamide (**19a**)

Greenish-white crystals (yield, 60%); m.p. = 262–263°C. IR (KBr, cm⁻¹): 3,324, 3,193 (NH, NH₂), 3,053 (CH aromatic), 2,953 (CH aliphatic), 1,685 (C=O), 1,593 (C=N), 1,252 (SO₂); ¹H NMR (DMSO-*d*₆) δ (ppm): 4.42 (s, 2H, SCH₂), 7.20 (br, s, 2H, exchangeable with D₂O, -NH₂), 7.61 (dd, 1H, $J = 7.5, 8.1$ Hz, Ar-H, H-8 of quinoxaline), 7.64 (dd, 1H, $J = 7.5, 8.1$ Hz, Ar-H, H-7 of quinoxaline), 7.73–7.79 (m, 4H, Ar-H, phenyl), 7.84 (d, 1H, $J = 7.5$ Hz, Ar-H, H-9 of quinoxaline), 8.28 (d, 1H, $J = 7.5$ Hz, Ar-H, H-6 of quinoxaline), 10.00 (s, 1H, Ar-H, N-CH=N), and 10.71 (s, 1H, exchangeable with D₂O, -NH); ¹³C NMR (DMSO-*d*₆, 100 MHz) δ (ppm): 34.35, 116.99, 119.40 (2C), 123.85, 123.91, 127.21 (2C), 128.34, 128.77, 135.54, 138.11, 139.06, 141.81, 142.26, 151.45, and 166.98; DEPT (DMSO-*d*₆, 100 MHz) δ (ppm): 34.36, 116.92, 116.99, 119.40, 127.21 (2C), 128.33, 128.35, 128.77, and 138.11; MS (*m/z*): 414 (M⁺, 8.9%), 335 (71%), and 169 (100% base peak); Anal. calcd. for C₁₇H₁₄N₆O₃S₂ (414.46): C, 49.27; H, 3.40; N, 20.28. Found: C, 49.59%; H, 3.69%; N, 20.92%.

2-[[1,2,4]Triazolo[4,3-*a*]quinoxalin-4-ylthio]-*N*-(4-(*N*-(pyridin-2-yl)sulfamoyl)phenyl)acetamide (**19b**)

Yellow crystals (yield, 65%); m.p. = 248–250°C. IR (KBr, cm⁻¹): 3,278, 3,182 (2NH), 3,049 (CH aromatic), 2,939 (CH aliphatic), 1,688 (C=O), 1,625 (C=N), and 1,152 (SO₂); ¹H NMR (DMSO-*d*₆) δ (ppm): 4.43 (s, 2H, SCH₂), 6.86 (dd, 1H, $J = 6.4$ Hz, H-5 of pyridine), 7.14 (d, 1H,

$J = 8.4$ Hz, H-3 of pyridine, 7.55–7.89 (m, 10H, Ar-H), 8.32 (s, 1H, Ar-H, N-CH=N), 10.04 (s, 1H, exchangeable with D_2O , -CONH), and 10.65 (s, 1H, exchangeable with D_2O , - SO_2NH); ^{13}C NMR (DMSO- d_6 , 100 MHz) δ (ppm): 34.92, 114.31, 116.98, 117.90, 118.87(2), 126.27, 128.29, 128.30(3), 128.23, 135.57, 138.21, 139.09, 140.79, 143.31, 143.36, 150.44, 151.62, 153.59, and 167.59; Anal. calcd. for $C_{22}H_{17}N_7O_3S_2$ (491.54): C, 53.76; H, 3.49; N, 19.95. Found: C, 53.99%; H, 3.88%; N, 20.35%.

2-([1,2,4]Triazolo[4,3-*a*]quinoxalin-4-ylthio)-*N*-(4-(*N*-(thiazol-2-yl)-sulfamoyl)phenyl)acetamide (19c)

Yellowish white crystals (yield, 70%); m.p. = 232–235°C. IR (KBr, cm^{-1}): 3,267, 3,185 (2NH), 3,108 (CH aromatic), 2,915 (CH aliphatic), 1,691 (C=O), 1,590 (C=N), and 1,138 (SO_2); 1H NMR (DMSO- d_6) δ (ppm): 4.41 (s, 2H, -SCH₂), 6.77 (d, 1H, $J = 4.8$ Hz, H-5 of thiazol), 7.19 (d, 1H, $J = 4.8$ Hz, H-4 of thiazol), 7.54–7.58 (m, 3H, Ar-H, H-7, H-8 and H-9 of quinoxaline), 7.67 (d, 2H, $J = 8.2$ Hz, Ar-H, H-3 and H-5 of phenyl), 7.73 (d, 2H, $J = 8.2$ Hz, Ar-H, H-2 and H-6 of phenyl), 7.79 (d, 1H, $J = 8$ Hz, Ar-H, H-6 of quinoxaline), 8.24 (s, 1H, Ar-H, N-CH=N), 10.00 (s, 1H, exchangeable with D_2O , CONH), and 10.68 (s, 1H, exchangeable with D_2O , - SO_2NH); ^{13}C NMR (DMSO- d_6 , 100 MHz) δ (ppm): 34.45, 108.48, 116.93, 119.29(2), 123.92, 124.98, 127.46(2), 128.20, 128.29, 128.60, 135.53, 137.41, 138.08, 141.84, 142.49, 151.51, 166.89, and 168.19; DEPT (DMSO- d_6 , 100 MHz) δ (ppm): 34.45, 108.47, 116.92, 119.38(2), 124.99, 127.47(2), 128.20, 128.29, 128.60, 138.08; MS (m/z): 497 (M^+ , 14.69%), 204.03 (45.39%), 155.23 (45.18%), and 78.64 (100% base peak); Anal. calcd. for $C_{20}H_{15}N_7O_3S_3$ (497.57): C, 48.28; H, 3.04; N, 19.71. Found: C, 48.58%; H, 3.44%; N, 20.05%.

3-([1,2,4]Triazolo[4,3-*a*]quinoxalin-4-ylthio)-*N*-(4-sulfamoylphenyl)propanamide (20)

Brown crystals (yield, 67%); m.p. = 264–265°C. IR (KBr, cm^{-1}): 3,240, 3,183 (NH, NH₂), 3,052 (CH aromatic), 2,925 (CH aliphatic), 1,680 (C=O), 1,592 (C=N), and 1,155 (SO_2); 1H NMR (DMSO- d_6) δ (ppm): 2.99 (t, 2H, $J = 6.5$ Hz, COCH₂), 3.67 (t, 2H, $J = 6.5$ Hz, -SCH₂), 7.25 (s, 2H, exchangeable with D_2O , -NH₂), 7.58 (dd, 1H, $J = 7.6, 8.4$ Hz, Ar-H, H-8 of quinoxaline), 7.63 (dd, 1H, $J = 7.6, 8.0$ Hz, Ar-H, H-7 of quinoxaline), 7.70 (d, 1H, $J = 8.4$ Hz, Ar-H, H-9 of quinoxaline), 7.75 (d, 1H, $J = 8.0$ Hz, Ar-H, H-6 of quinoxaline), 7.79 (d, 2H, $J = 8.0$ Hz, Ar-H, H-2, and H-6 of phenyl), 7.91 (d, 2H, $J = 8.0$ Hz, Ar-H, H-3, and H-5 of phenyl), 8.30 (s, 1H, Ar-H, N-CH=N), and 10.05 (s, 1H, exchangeable with D_2O , -NH); ^{13}C NMR (DMSO- d_6 , 100 MHz) δ (ppm): 24.21, 36.08, 116.93, 119.07(2), 123.85, 127.17(3), 128.16, 128.50, 135.66, 138.14, 138.76, 142.01, 142.35, 151.95, and 170.38; DEPT (DMSO- d_6 , 100 MHz) δ (ppm): 24.21, 36.09 (2CH₂), 116.92, 119.06(2), 127.17(3), 128.16, and 128.49(2); Anal. calcd. for $C_{18}H_{16}N_6O_3S_2$ (428.49): C, 50.46; H, 3.76; N, 19.61. Found: C, 50.11%; H, 3.31%; N, 19.02%.

2-([1,2,4]Triazolo[4,3-*a*]quinoxalin-4-ylthio)-*N*-(4-sulfamoylbenzyl)acetamide (21)

Yellow crystals (yield, 60%); m.p. = 215–217°C. IR (KBr, cm^{-1}): 3,310, 3,180 (NH, NH₂), 3,079 (CH aromatic), 2,925 (CH aliphatic), 1,685

(C=O), 1,597 (C=N), and 1,136 (SO_2); 1H NMR (DMSO- d_6) δ (ppm): 4.24 (s, 2H, SCH₂), 4.40 (s, 2H, -NHCH₂), 7.30 (br, s, 2H, exchangeable with D_2O , -NH₂), 7.43 (d, 2H, Ar-H, $J = 7.88$ Hz, H-3, and H-5 of phenyl), 7.62 (dd, 1H, $J = 7.5, 8.1$ Hz, Ar-H, H-8 of quinoxaline), 7.68 (dd, 1H, $J = 7.5, 8.0$ Hz, Ar-H, H-7 of quinoxaline), 7.70 (d, 2H, Ar-H, $J = 7.88$ Hz, H-2, and H-6 of phenyl), 7.86 (d, 1H, $J = 8.1$ Hz, Ar-H, H-9 of quinoxaline), 8.34 (d, 1H, $J = 8.0$ Hz, Ar-H, H-6 of quinoxaline), 8.90 (s, 1H, Ar-H, N-CH=N), and 10.09 (s, 1H, exchangeable with D_2O , -NH); ^{13}C NMR (DMSO- d_6 , 100 MHz) δ (ppm): 32.93, 42.75, 117.04, 123.97, 126.07 (2C), 127.83 (2C), 128.26, 128.44, 128.71, 135.56, 138.21, 141.90, 143.05, 143.79, 151.66, and 167.56; DEPT (DMSO- d_6 , 100 MHz) δ (ppm): 32.93, 42.75, 117.03, 126.06 (2C), 127.82 (2C), 128.25, 128.44, 128.70, and 138.21; Anal. calcd. for $C_{18}H_{16}N_6O_3S_2$ (428.49): C, 50.46; H, 3.76; N, 19.61. Found: C, 50.78%; H, 3.44%; N, 19.85%.

2-([1,2,4]Triazolo[4,3-*a*]quinoxalin-4-ylthio)acetamide (22)

Beige yellow crystals (yield, 70%); m.p. = 255–256°C. IR (KBr, cm^{-1}): 3,197, 3,120 (NH₂), 3,066 (CH aromatic), 2,925 (CH aliphatic), 1,667 (C=O), and 1,624 (C=N); 1H NMR (DMSO- d_6) δ (ppm): 4.13 (s, 2H, CH₂), 7.27 (s, 2H, exchangeable with D_2O , -NH₂), 7.64 (dd, 1H, $J = 7.5, 8.1$ Hz, Ar-H, H-8 of quinoxaline), 7.71 (dd, 1H, $J = 7.5, 8.1$ Hz, Ar-H, H-7 of quinoxaline), 7.92 (d, 1H, $J = 8.1$ Hz, Ar-H, H-9 of quinoxaline), 8.34 (d, 1H, $J = 7.5$ Hz, Ar-H, H-6 of quinoxaline), and 10.10 (s, 1H, Ar-H, N-CH=N); ^{13}C NMR (DMSO- d_6 , 100 MHz) δ (ppm): 33.01, 117.07, 124.00, 128.30, 128.49, 128.66, 135.63, 138.21, 141.93, 151.78, and 169.22; DEPT (DMSO- d_6 , 100 MHz) δ (ppm): 33.01 (1CH₂), 117.07, 128.30, 128.49, 128.66, and 138.22 (5CH); MS (m/z): 259 (M^+ , 24.08%), 212 (48.79%), 202.60 (14.16%), and 96.75 (100% base peak); Anal. calcd. for $C_{11}H_9N_5OS$ (259.29): C, 50.96; H, 3.50; N, 27.01. Found: C, 50.61%; H, 3.11%; N, 27.42%.

2-([1,2,4]Triazolo[4,3-*a*]quinoxalin-4-ylthio)-*N*-(4-acetylphenyl)acetamide (23)

Brown powder (yield, 75%); m.p. = 117–118°C. IR (KBr, cm^{-1}): 3,248 (NH), 3,045 (CH aromatic), 2,900 (CH aliphatic), 1,675 (C=O), and 1,594 (C=N); 1H NMR (DMSO- d_6) δ (ppm): 2.66 (s, 3H, -COCH₃), 4.45 (s, 2H, CH₂), 7.55 (dd, 1H, $J = 7.4, 8.0$ Hz, Ar-H, H-8 of quinoxaline), 7.62 (dd, 1H, $J = 7.4, 8.6$ Hz, Ar-H, H-7 of quinoxaline), 7.79 (d, 1H, $J = 8.0$ Hz, Ar-H, H-9 of quinoxaline), 7.82 (d, 1H, $J = 8.6$ Hz, Ar-H, H-6 of quinoxaline), 7.99 (d, 2H, $J = 7.5$ Hz, Ar-H, H-2, and H-6 of phenyl), 8.35 (d, 2H, $J = 7.5$ Hz, Ar-H, H-3, and H-5 of phenyl), 10.10 (s, 1H, Ar-H, N-CH=N), and 10.80 (s, 1H, exchangeable with D_2O , -NH); ^{13}C NMR (DMSO- d_6 , 100 MHz) δ (ppm): 27.60, 34.52, 116.16, 118.88, 119.05(2), 123.34, 126.21, 128.26, 129.62(2), 135.56, 138.22, 143.42, 146.72, 151.57, 166.90, 170.25, and 196.88; Anal. calcd. for $C_{19}H_{15}N_5O_2S$ (377.42): C, 60.47; H, 4.01; N, 18.56. Found: C, 60.22%; H, 4.41%; N, 18.92%.

4.1.5 | General procedure for the synthesis of compounds 24a–g

A mixture of the potassium salt **17** (2.94 g, 0.01 mol) and the different alkyl halids (0.025 mol), namely, methyl bromide, ethyl

bromide, *n*-butyl bromide, *n*-hexyl bromide, *n*-decyl bromide, allyl bromide, and benzyl bromide in dry DMF (40 ml) was heated on a water bath for 4 hr. After cooling, the reaction mixture was poured onto ice water (300 ml) with continuous stirring. The formed precipitate was filtered, washed with water, and crystallized from ethanol to afford the corresponding compounds **24a–g**, respectively.

5-Methyl-1-(methylthio)-[1,2,4]triazolo[4,3-*a*]quinoxalin-4(5H)-one (24a)

Beige crystals (yield, 75%); m.p. = 159–160°C. IR (KBr, cm^{-1}): 3,070 (CH aromatic), 2,915 (CH aliphatic), 1,689 (C=O), and 1,596 (C=N); ^1H NMR (DMSO- d_6) δ (ppm): 2.71 (s, 3H, SCH₃), 2.92 (s, 3H, NCH₃), 7.58 (dd, 1H, *J* = 7.8, 8.0 Hz, Ar-H, H-8 of quinoxaline), 7.63 (dd, 1H, *J* = 7.8, 8.2 Hz, Ar-H, H-7 of quinoxaline), 7.88 (d, 1H, *J* = 8.2 Hz, Ar-H, H-6 of quinoxaline), and 8.41 (d, 1H, *J* = 7.8 Hz, Ar-H, H-9 of quinoxaline); ^{13}C NMR (DMSO- d_6 , 100 MHz) δ (ppm): 11.76, 16.53, 116.24, 125.15, 127.95, 128.02, 128.72, 136.34, 144.33, 148.22, and 153.23; DEPT (DMSO- d_6 , 100 MHz) δ (ppm): 13.15, 17.93 (2CH₃), 117.66, 129.44, 130.14, and 136.34 (4CH); Anal. calcd. for C₁₁H₁₀N₄OS (246.29): C, 53.64; H, 4.09; N, 22.75. Found: C, 53.98%; H, 4.41%; N, 22.42%.

5-Ethyl-1-(ethylthio)-[1,2,4]triazolo[4,3-*a*]quinoxalin-4(5H)-one (24b)

Yellow crystals (yield, 70%); m.p. = 173–175°C. IR (KBr, cm^{-1}): 3,065 (CH aromatic), 2,915 (CH aliphatic), 1,687 (C=O), and 1,590 (C=N); ^1H NMR (DMSO- d_6) δ (ppm): 1.39 (t, 3H, SCH₂CH₃), 1.43 (t, 3H, NCH₂CH₃), 3.25 (q, 2H, SCH₂CH₃), 3.41 (q, 2H, NCH₂CH₃), 7.55 (dd, 1H, *J* = 6.8, 8.5 Hz, Ar-H, H-8 of quinoxaline), 7.58 (dd, 1H, *J* = 6.8, 8.1 Hz, Ar-H, H-7 of quinoxaline), 7.82 (d, 1H, *J* = 8.1 Hz, Ar-H, H-6 of quinoxaline), 8.44 (d, 1H, *J* = 8.5 Hz, Ar-H, H-9 of quinoxaline); ^{13}C NMR (DMSO- d_6 , 100 MHz) δ (ppm): 14.60, 14.98, 23.12, 28.57, 116.31, 125.17, 127.92, 127.95, 128.66, 136.31, 144.06, 147.11, and 152.63; DEPT (DMSO- d_6 , 100 MHz) δ (ppm): 14.60, 14.98 (2CH₃), 22.89, 28.56 (2CH₂), 116.31, 127.92, 127.95, and 128.67 (4CH); Anal. calcd. for C₁₃H₁₄N₄OS (274.34): C, 56.92; H, 5.14; N, 20.42. Found: C, 56.65%; H, 5.49%; N, 20.77%.

5-Butyl-1-(butylthio)-[1,2,4]triazolo[4,3-*a*]quinoxalin-4(5H)-one (24c)

Yellow crystals (yield, 68%); m.p. = 205–207°C. IR (KBr, cm^{-1}): 3,089 (CH aromatic), 2,935 (CH aliphatic), 1,687 (C=O), and 1,583 (C=N); ^1H NMR (DMSO- d_6) δ (ppm): 0.82 (t, 3H, SCH₂CH₂CH₂CH₃), 0.98 (t, 3H, NCH₂CH₂CH₂CH₃), 1.44–1.53 (m, 4H, SCH₂CH₂CH₂CH₃, and NCH₂CH₂CH₂CH₃), 1.73–1.80 (m, 4H, SCH₂CH₂CH₂CH₃, and NCH₂CH₂CH₂CH₃), 3.34 (t, 2H, SCH₂CH₂CH₂CH₃), 3.43 (t, 2H, NCH₂CH₂CH₂CH₃), 7.55 (dd, 1H, *J* = 7.3, 8.0 Hz, Ar-H, H-8 of quinoxaline), 7.59 (dd, 1H, *J* = 7.3, 8.1 Hz, Ar-H, H-7 of quinoxaline), 7.85 (d, 1H, *J* = 8.1 Hz, Ar-H, H-6 of quinoxaline), and 8.55 (d, 1H, *J* = 8.0 Hz, Ar-H, H-9 of quinoxaline); ^{13}C NMR (DMSO- d_6 , 100 MHz) δ (ppm): 13.74, 13.86, 21.62, 21.91, 28.25, 31.12, 31.27, 33.91, 116.35, 125.27, 127.91, 127.94, 128.67, 136.40, 144.14, 147.29, and 152.84; DEPT (DMSO- d_6 , 100 MHz) δ (ppm): 13.74, 13.86 (2CH₃), 21.62,

21.91, 28.25, 31.12, 31.27, 33.91 (6CH₂), 116.35, 127.91, 127.94, and 28.67 (4CH); Anal. calcd. for C₁₇H₂₂N₄OS (330.45): C, 61.79; H, 6.71; N, 16.96. Found: C, 61.55%; H, 6.45%; N, 16.72%.

5-Hexyl-1-(hexylthio)-[1,2,4]triazolo[4,3-*a*]quinoxalin-4(5H)-one (24d)

Yellow crystals (yield, 65%); m.p. = 199–201°C. IR (KBr, cm^{-1}): 3,069 (CH aromatic), 2,920 (CH aliphatic), 1,691 (C=O), and 1,592 (C=N); ^1H NMR (DMSO- d_6) δ (ppm): 0.82 (t, 3H, SCH₂CH₂CH₂CH₂CH₂CH₃), 0.86 (t, 3H, NCH₂CH₂CH₂CH₂CH₂CH₃), 1.23–1.41 (m, 12H, SCH₂CH₂CH₂CH₂CH₂CH₃, and NCH₂CH₂CH₂CH₂CH₂CH₃), 1.72–1.81 (m, 4H, SCH₂CH₂CH₂CH₂CH₂CH₃, and NCH₂CH₂CH₂CH₂CH₂CH₃), 3.34 (t, 2H, *J* = 9.20 Hz, SCH₂CH₂CH₂CH₂CH₃), 3.44 (t, 2H, *J* = 7.20 Hz, NCH₂CH₂CH₂CH₂CH₃), 7.37 (dd, 1H, *J* = 7.5, 8.0 Hz, Ar-H, H-8 of quinoxaline), 7.54 (dd, 1H, *J* = 7.5, 8.1 Hz, Ar-H, H-7 of quinoxaline), 7.59 (d, 1H, *J* = 8.1 Hz, Ar-H, H-6 of quinoxaline), and 8.14 (d, 1H, *J* = 8.0 Hz, Ar-H, H-9 of quinoxaline); ^{13}C NMR (DMSO- d_6 , 100 MHz) δ (ppm): 14.18, 14.30, 22.35 (2C), 22.43, 28.12, 28.40, 28.56, 29.13, 31.12 (2C), 31.18, 39.40, 40.85, 116.31, 116.88, 125.18, 127.88, 128.17, 128.60, and 136.34; Anal. calcd. for C₂₁H₃₀N₄OS (386.56): C, 65.25; H, 7.82; N, 14.49. Found: C, 65.15%; H, 7.66%; N, 14.87%.

5-Decyl-1-(decylthio)-[1,2,4]triazolo[4,3-*a*]quinoxalin-4(5H)-one (24e)

Greenish-white crystals (yield, 60%); m.p. = 80–81°C. IR (KBr, cm^{-1}): 3,078 (CH aromatic), 2,920 (CH aliphatic), 1,688 (C=O), and 1,603 (C=N); ^1H NMR (DMSO- d_6) δ (ppm): 0.84–0.87 (m, 6H, 2CH₃), 1.23–1.26 (m, 24H, 12CH₂), 1.38–1.42 (m, 4H, 2CH₂), 1.75–1.78 (m, 4H, 2CH₂), 3.26 (t, 2H, SCH₂), 3.38 (t, 2H, NCH₂), 7.23 (dd, 1H, *J* = 6.5, 8.0 Hz, Ar-H, H-8 of quinoxaline), 7.32 (dd, 1H, *J* = 6.5, 8.5 Hz, Ar-H, H-7 of quinoxaline), 7.72 (d, 1H, *J* = 8.5 Hz, Ar-H, H-6 of quinoxaline), 8.32 (d, 1H, *J* = 8.0 Hz, Ar-H, H-9 of quinoxaline); ^{13}C NMR (DMSO- d_6 , 100 MHz) δ (ppm): 14.28 (2C), 22.47 (2C), 25.94, 29.08 (2C), 29.37 (3C), 29.41 (3C), 29.45 (2C), 29.49, 31.70 (2C), 61.23 (2C), 116.30, 116.84, 125.13, 125.18, 127.80, 127.86, 128.10, 128.55, and 136.30; DEPT (DMSO- d_6 , 100 MHz) δ (ppm): 14.28, 22.47 (2CH₃), 25.94(2), 29.04, 29.09(2), 29.30(2), 29.39, 29.44(2), 29.48(2), 31.70(2), 32.99(2), 61.23(2) (18CH₂), 116.30, 127.80, 127.86, and 128.10 (4CH); Anal. calcd. for C₂₉H₄₆N₄OS (498.77): C, 69.84; H, 9.30; N, 11.23. Found: C, 69.53%; H, 9.68%; N, 11.61%.

5-Allyl-1-(allylthio)-[1,2,4]triazolo[4,3-*a*]quinoxalin-4(5H)-one (24f)

Yellowish white crystals (yield, 73%); m.p. = 210–212°C. IR (KBr, cm^{-1}): 3,067 (CH aromatic), 2,920 (CH aliphatic), 1,692 (C=O), and 1,591 (C=N); ^1H NMR (DMSO- d_6) δ (ppm): 3.97 (d, 2H, *J* = 8 Hz, SCH₂), 4.08 (d, 2H, *J* = 8.5, NCH₂), 5.13–5.22 (m, 4H, 2CH₂), 5.96–6.08 (m, 2H, 2CH₂CH = CH₂), 7.48 (dd, 1H, *J* = 6.4, 8.8 Hz, Ar-H, H-8 of quinoxaline), 7.55 (dd, 1H, *J* = 6.4, 8.4 Hz, Ar-H, H-7 of quinoxaline), 7.77 (d, 1H, *J* = 8.4 Hz, Ar-H, H-6 of quinoxaline), and 8.41 (d, 1H, *J* = 8.8 Hz, Ar-H, H-9 of quinoxaline); ^{13}C NMR (DMSO- d_6 , 100 MHz) δ (ppm): 31.27, 36.80, 116.24, 119.27, 119.85, 125.03, 127.89, 128.02, 128.60, 133.03, 133.45, 136.06, 143.89, 146.50, and 151.77; DEPT (DMSO- d_6 , 100 MHz) δ (ppm): 31.26, 36.80, 116.24,

119.26, 119.84 (4CH₂), 127.89, 128.02, 128.60, 133.03, and 133.45 (6CH); Anal. calcd. for C₁₅H₁₄N₄O₅S (298.36): C, 60.38; H, 4.73; N, 18.78. Found: C, 60.73%; H, 4.38%; N, 18.41%.

5-Benzyl-1-(benzylthio)-[1,2,4]triazolo[4,3-a]quinoxalin-4(5H)-one (24g)

Beige crystals (yield, 66%); m.p. = 188–190°C. IR (KBr, cm⁻¹): 3,073 (CH aromatic), 2,935 (CH aliphatic), 1,693 (C=O), and 1,597 (C=N); ¹H NMR (DMSO-*d*₆) δ ppm: 4.62 (s, 2H, SCH₂), 4.70 (s, 2H, NCH₂), 7.22–7.40 (m, 6H, Ar-H, H-3, H-4, and H-5 of two phenyl), 7.45 (dd, 1H, *J* = 7.4, 8.2 Hz, Ar-H, H-8 of quinoxaline), 7.55 (dd, 1H, *J* = 7.4, 8.1 Hz, Ar-H, H-7 of quinoxaline), 7.57–7.60 (m, 4H, Ar-H, H-2, H-6 of two phenyl), 7.94 (d, 1H, *J* = 8.1 Hz, Ar-H, H-6 of quinoxaline), 8.41 (d, 1H, *J* = 8.2 Hz, Ar-H, H-9 of quinoxaline); ¹³C NMR (DMSO-*d*₆, 100 MHz) δ (ppm): 32.46, 38.15, 116.52, 125.28, 127.71, 128.10, 128.13, 128.24, 128.75, 128.89, 128.94, 128.97(2), 129.65(2), 129.70(2), 129.75, 136.21, 136.72, 137.80, 143.96, 146.82, and 151.91; DEPT (DMSO-*d*₆, 100 MHz) δ (ppm): 32.46, 38.15 (2CH₂), 116.52, 127.70, 128.11, 128.23, 128.75, 128.89(2), 128.93(2), 129.64(2), and 129.74(3) (14CH); Anal. calcd. for C₂₃H₁₈N₄O₅S (398.48): C, 69.33; H, 4.55; N, 14.06. Found: C, 69.03%; H, 4.98%; N, 14.51%.

4.1.6 | General procedure for the synthesis of compounds 25a–d and 26

A mixture of the dipotassium salt **17** (2.94 g, 0.01 mol) and the appropriate 2-chloroacetate or 2-chloropropanoate derivatives (0.025 mol), namely, methyl 2-chloroacetate, ethyl 2-chloroacetate, isopropyl 2-chloroacetate and isobutyl 2-chloroacetate, and methyl 2-chloropropanoate in dry DMF (40 ml) was heated on a water bath for 2 hr. After cooling, the reaction mixture was poured onto ice water (300 ml). Then, DCM (100 ml) was added. The organic layer was separated using separating funnel, dried over anhydrous NaSO₄, and evaporated under vacuum. The formed precipitate was crystallized from ethanol to afford the corresponding compounds **25a–d**, and **26**, respectively.

Methyl 2-((5-(2-methoxy-2-oxoethyl)-4-oxo-4,5-dihydro-[1,2,4]triazolo[4,3-a]quinoxalin-1-yl)thio)acetate (25a)

White powder (yield, 80%); m.p. = 155–157°C. IR (KBr, cm⁻¹): 3,089 (CH aromatic), 2,930 (CH aliphatic), 1,735 (C=O), and 1,586 (C=N); ¹H NMR (DMSO-*d*₆) δ (ppm): 3.67 (s, 3H, OCH₃), 3.73 (s, 3H, OCH₃), 4.27 (s, 2H, SCH₂), 4.40 (s, 2H, NCH₂), 7.57 (dd, 1H, *J* = 6.4, 7.8 Hz, Ar-H, H-8 of quinoxaline), 7.61 (dd, 1H, *J* = 6.4, 8.0 Hz, Ar-H, H-7 of quinoxaline), 7.78 (d, 1H, *J* = 8.0 Hz, Ar-H, H-6 of quinoxaline), and 8.41 (d, 1H, *J* = 7.8 Hz, Ar-H, H-9 of quinoxaline); ¹³C NMR (DMSO-*d*₆, 100 MHz) δ (ppm): 31.28, 35.99, 52.91, 53.03, 116.39, 125.03, 128.18, 128.47, 128.67, 135.96, 143.90, 146.57, 151.23, 168.70, and 169.23; DEPT (DMSO-*d*₆, 100 MHz) δ (ppm): 31.28, 35.89 (2CH₃), 52.91, 53.03 (CH₂), 116.39, 128.19, 128.48, and 128.68 (4CH); MS (*m/z*): 362 (M⁺, 1.7%), 319 (100% base peak), 287 (11.54%), and 188

(10.25%); Anal. calcd. for C₁₅H₁₄N₄O₅S (362.36): C, 49.72; H, 3.89; N, 15.46. Found: C, 49.44%; H, 3.58%; N, 15.81%.

Ethyl 2-((5-(2-ethoxy-2-oxoethyl)-4-oxo-4,5-dihydro-[1,2,4]triazolo[4,3-a]quinoxalin-1-yl)thio)acetate (25b)

Yellowish white crystals (yield, 77%); m.p. = 148–150°C. IR (KBr, cm⁻¹): 3,081 (CH aromatic), 2,933 (CH aliphatic), 1,734 (C=O), and 1,590 (C=N); ¹H NMR (DMSO-*d*₆) δ (ppm): 1.14 (t, 3H, *J* = 7.5 Hz, CH₂CH₃), 1.22 (t, 3H, *J* = 7 Hz, CH₂CH₃), 4.09 (q, 2H, *J* = 7.5 Hz, CH₂CH₃), 4.16 (q, 2H, *J* = 7 Hz, CH₂CH₃), 4.24 (s, 2H, SCH₂), 4.39 (s, 2H, NCH₂), 7.58 (dd, 1H, *J* = 6.4, 8.1 Hz, Ar-H, H-8 of quinoxaline), 7.64 (dd, 1H, *J* = 6.4, 8.1 Hz, Ar-H, H-7 of quinoxaline), 7.77 (d, 1H, *J* = 8.1 Hz, Ar-H, H-6 of quinoxaline), and 8.41 (d, 1H, *J* = 8.1 Hz, Ar-H, H-9 of quinoxaline); ¹³C NMR (DMSO-*d*₆, 100 MHz) δ (ppm): 14.35, 14.56, 31.57, 36.10, 61.67, 61.91, 116.45, 125.03, 128.24, 128.50, 128.63, 135.94, 143.85, 146.65, 151.33, 168.24, and 168.70; DEPT (DMSO-*d*₆, 100 MHz) δ (ppm): 14.36, 14.57 (2CH₃), 31.58, 36.11, 61.67, 61.91 (4CH₂), 116.44, 128.24, 128.50, and 128.63 (4CH); Anal. calcd. for C₁₇H₁₈N₄O₅S (390.41): C, 52.30; H, 4.65; N, 14.35. Found: C, 52.63%; H, 4.28%; N, 14.71%.

Isopropyl 2-((5-(2-isopropoxy-2-oxoethyl)-4-oxo-4,5-dihydro-[1,2,4]triazolo[4,3-a]quinoxalin-1-yl)thio)acetate (25c)

Yellow crystals (yield, 60%); m.p. = 141–143°C. IR (KBr, cm⁻¹): 3,079 (CH aromatic), 2,983 (CH aliphatic), 1,735 (C=O), and 1,586 (C=N); ¹H NMR (DMSO-*d*₆) δ ppm: 1.12 (d, 6H, *J* = 6.40 Hz, 2CH₃), 1.23 (d, 6H, *J* = 6.40 Hz, 2CH₃), 4.23 (s, 2H, SCH₂), 4.32 (s, 2H, -NHCH₂), 4.91 (m, 1H, -CH), 4.98 (m, 1H, -CH), 7.64 (dd, 1H, *J* = 7.5, 8.1 Hz, Ar-H, H-8 of quinoxaline), 7.70 (dd, 1H, *J* = 7.5, 8.0 Hz, Ar-H, H-7 of quinoxaline), 7.85 (d, 1H, *J* = 8.0 Hz, Ar-H, H-6 of quinoxaline), and 8.58 (d, 1H, *J* = 8.1 Hz, Ar-H, H-9 of quinoxaline); ¹³C NMR (DMSO-*d*₆, 100 MHz) δ (ppm): 21.80 (2C), 21.97 (2C), 31.86, 36.58, 69.23, 69.57, 116.64, 125.24, 128.35, 128.56, 128.71, 136.14, 143.93, 151.51, 167.63, and 168.08 (2C); DEPT (DMSO-*d*₆, 100 MHz) δ (ppm): 21.80 (2C), 21.97 (2C), 31.86, 36.57, 69.23, 69.57, 116.64, 128.35, 128.56, and 128.71; Anal. calcd. for C₁₉H₂₂N₄O₅S (418.47): C, 54.53; H, 5.30; N, 13.39. Found: C, 54.88%; H, 5.44%; N, 13.85%.

Isobutyl 2-((5-(2-isobutoxy-2-oxoethyl)-4-oxo-4,5-dihydro-[1,2,4]triazolo[4,3-a]quinoxalin-1-yl)thio)acetate (25d)

Yellow crystals (yield, 60%); m.p. = 120–121°C. IR (KBr, cm⁻¹): 3,079 (CH aromatic), 2,983 (CH aliphatic), 1,735 (2C=O), and 1,586 (C=N); ¹H NMR (DMSO-*d*₆) δ (ppm): 0.78 (t, 6H, *J* = 6.5 Hz, CH (CH₃)₂), 0.87 (t, 6H, *J* = 6.5 Hz, CH (CH₃)₂), 1.78–1.83 (m, 1H, -CH(CH₃)₂), 1.88–1.91 (m, 1H, -CH(CH₃)₂), 3.82 (d, 2H, *J* = 7 Hz, Hz, OCH₂), 3.92 (d, 2H, *J* = 6.5 Hz, OCH₂), 4.26 (s, 2H, SCH₂), 4.37 (s, 2H, NCH₂), 7.63 (dd, 1H, *J* = 7.4, 8.5 Hz, Ar-H, H-8 of quinoxaline), 7.70 (dd, 1H, *J* = 7.4, 8.1 Hz, Ar-H, H-7 of quinoxaline), 7.82 (d, 1H, *J* = 8.1 Hz, Ar-H, H-6 of quinoxaline), 8.51 (d, 1H, *J* = 8.5 Hz, Ar-H, H-9 of quinoxaline); ¹³C NMR (DMSO-*d*₆, 100 MHz) δ (ppm): 19.07(2), 19.19(2), 27.64, 27.72, 31.44, 36.11, 71.40, 71.55, 116.52, 125.13, 128.30, 128.58, 128.67, 136.08, 143.93, 146.67, 151.41, 168.18, 168.54; DEPT (DMSO-*d*₆, 100 MHz) δ (ppm): 19.07(2), 19.19(2) (4CH₃), 27.64,

27.72, 31.44, 36.11 (4CH₂), 71.40, 71.55, 116.52, 128.30, 128.58, 128.67 (6CH); Anal. calcd. for C₂₁H₂₆N₄O₅S (446.52): C, 56.49; H, 5.87; N, 12.55. Found: C, 56.12%; H, 5.55%; N, 13.01%.

Methyl 2-((5-(1-methoxy-1-oxopropan-2-yl)-4-oxo-4,5-dihydro-[1,2,4]triazolo[4,3-a]quinoxalin-1-yl)thio)propanoate (26)

Yellow crystals (yield, 70%); m.p. = 173–175°C. IR (KBr, cm⁻¹): 3,053 (CH aromatic), 2,953 (CH aliphatic), 1,742 (C=O), and 1,593 (C=N); ¹H NMR (DMSO-*d*₆) δ ppm: 1.60 (d, 3H, *J* = 7.20 Hz, SCHCH₃), 1.67 (d, 3H, *J* = 7.20 Hz, NCHCH₃), 3.55 (s, 3H, OCH₃), 3.73 (s, 3H, OCH₃), 4.53 (q, 1H, *J* = 7.20 Hz, SCHCH₃), 4.76 (q, 1H, *J* = 7.20 Hz, SCHCH₃), 7.57 (dd, 1H, *J* = 7.2, 8.4 Hz, Ar-H, H-8 of quinoxaline), 7.76 (dd, 1H, *J* = 7.4, 8.0 Hz, Ar-H, H-7 of quinoxaline), 7.78 (d, 1H, *J* = 8.0 Hz, Ar-H, H-6 of quinoxaline), and 8.65 (d, 1H, *J* = 8.4 Hz, Ar-H, H-9 of quinoxaline); ¹³C NMR (DMSO-*d*₆, 100 MHz) δ (ppm): 17.62, 17.96, 40.94, 45.78, 53.04, 53.10, 116.43, 125.19, 128.33, 128.53, 128.64, 136.03, 143.65, 144.80, 150.91, 171.40, and 172.20; DEPT (DMSO-*d*₆, 100 MHz) δ (ppm): 17.62, 17.96, 53.04, 53.10 (4CH₃), 40.94, 45.78, 116.43, 128.33, 128.53, and 128.64 (6CH); Anal. calcd. for C₁₇H₁₈N₄O₅S (390.41): C, 52.30; H, 4.65; N, 14.35. Found: C, 52.62%; H, 5.05%; N, 14.05%.

4.1.7 | General procedure for the synthesis of compounds 27 and 28a,b

A mixture of the dipotassium salt 17 (2.94 g, 0.01 mol) and the appropriate 2-chloroacetamido derivatives (0.02 mol), namely, 4-(2-chloroacetamido)benzoic acid, 2-chloro-*N*-(4-sulfamoylphenyl)acetamide, and 2-chloro-*N*-(4-(*N*-(pyridin-2-yl)sulfamoyl)phenyl)acetamide in dry DMF (30 ml) was heated on a water bath for 4 hr. After cooling, the reaction mixture was poured onto ice water (250 ml) with continuous stirring. The formed precipitate was filtered, washed with water, and crystallized from ethanol to afford the corresponding compounds 27 and 28a,b, respectively.

4-(2-((5-(2-((4-Carboxyphenyl)amino)-2-oxoethyl)-4-oxo-4,5-dihydro-[1,2,4]triazolo[4,3-a]quinoxalin-1-yl)thio)acetamido)benzoic acid (27)

Beige crystal (yield, 60%); m.p. = 267–278°C. IR (KBr, cm⁻¹): 3,590 (OH), 3,082 (CH aromatic), 2,920 (CH aliphatic), 1,685 (C=O), and 1,601 (C=N); ¹H NMR (DMSO-*d*₆) δ (ppm): 4.31 (s, 2H, SCH₂), 4.44 (s, 2H, NCH₂), 7.46 (dd, 1H, *J* = 7.5, 8.1 Hz, Ar-H, H-8 of quinoxaline), 7.59 (dd, 1H, *J* = 7.5, 8.1 Hz, Ar-H, H-7 of quinoxaline), 7.70 (d, 1H, *J* = 8.1 Hz, Ar-H, H-6 of quinoxaline), 7.84–7.89 (m, 8H, Ar-H, phenyl), 8.39 (d, 1H, *J* = 8.1 Hz, Ar-H, H-9 of quinoxaline), 10.67 (s, 1H, exchangeable with D₂O, -SCONH), 10.74 (s, 1H, exchangeable with D₂O, -NCONH), and 12.73 (br s, 2H, exchangeable with D₂O, 2OH); ¹³C NMR (DMSO-*d*₆, 100 MHz) δ (ppm): 34.48, 49.06, 118.96(4), 124.96, 125.83, 125.94, 128.07, 128.29, 128.52, 130.38(2), 130.88(2), 135.94, 143.00, 143.30, 143.83, 146.81, 151.66, 166.14, 166.89, 167.37, and 167.40(2); MS (*m/z*): 572 (M⁺, 26.25%), 551 (100% base peak), 396 (56.61%), and 216 (20%); Anal. calcd. for

C₂₇H₂₀N₆O₇S (572.55): C, 56.64; H, 3.52; N, 14.68. Found: C, 56.92%; H, 3.95%; N, 15.01%.

2-(4-Oxo-1-((2-oxo-2-((4-sulfamoylphenyl)amino)ethyl)thio)-[1,2,4]-triazolo[4,3-a]quinoxalin-5(4H)-yl)-*N*-(4-sulfamoylphenyl)acetamide (28a)

Brown crystals (yield, 82%); m.p. = 230–231°C. IR (KBr, cm⁻¹): 3,254, 3,190 (NH₂ and 2NH overlapped), 3,056 (CH aromatic), 2,924 (CH aliphatic), 1,675 (C=O), 1,594 (C=N), and 1,154 (SO₂); ¹H NMR (DMSO-*d*₆) δ ppm: 3.73 (s, 2H, SCH₂), 4.43 (s, 2H, NCH₂), 7.34 (br, s, 4H, exchangeable with D₂O, 2NH₂), 7.10–7.22 (m, 8H, Ar-H, of 2 phenyl), 7.40 (dd, 1H, *J* = 7.5, 8.0 Hz, Ar-H, H-8 of quinoxaline), 7.41 (dd, 1H, *J* = 7.5, 8.1 Hz, Ar-H, H-7 of quinoxaline), 7.56 (d, 1H, *J* = 8.1 Hz, Ar-H, H-6 of quinoxaline), 8.14 (d, 1H, *J* = 8.0 Hz, Ar-H, H-9 of quinoxaline), 10.77 (s, 1H, exchangeable with D₂O, -SCONH), and 10.85 (s, 1H, exchangeable with D₂O, -NCONH); ¹³C NMR (DMSO-*d*₆, 100 MHz) δ (ppm): 34.28, 51.06, 119.36 (4C), 127.28 (4C), 128.37 (2C), 128.63, 136.01 (2C), 133.00, 137.32, 139.01, 142.02, 142.32, 146.87, 155.06, 159.05, and 167.05 (2C); DEPT (DMSO-*d*₆, 100 MHz) δ (ppm): 34.38, 51.06, 119.36 (4C), 127.30 (4C), 128.26, 128.56, 133.00, and 137.32. Anal. calcd. for C₂₅H₂₂N₆O₇S₃ (642.68): C, 46.72; H, 3.45; N, 17.44. Found: C, 46.44%; H, 3.05%; N, 17.91%.

2-(4-Oxo-1-((2-oxo-2-((4-(*N*-(pyridin-2-yl)sulfamoyl)phenyl)amino)ethyl)thio)-[1,2,4]triazolo[4,3-a]quinoxalin-5(4H)-yl)-*N*-(4-(*N*-(pyridin-2-yl)sulfamoyl)phenyl)acetamide (28b)

Brown powder (yield, 75%); m.p. = 228–229°C. IR (KBr, cm⁻¹): 3,293 (NH), 3,039 (CH aromatic), 2,965 (CH aliphatic), 1,687 (C=O), 1,592 (C=N), and 1,136 (SO₂); ¹H NMR (DMSO-*d*₆) δ (ppm): 4.37 (s, 2H, SCH₂), 4.45 (s, 2H, NCH₂), 6.81–6.85 (m, 2H, Ar-H), 7.12 (d, 2H, Ar-H), 7.61–8.05 (m, 13H, Ar-H), 8.37 (d, 2H, Ar-H), 10.22 (s, 1H, exchangeable with D₂O, -SCONH), 10.53 (s, 2H, exchangeable with D₂O, -NCONH), and 10.98 (s, 2H, exchangeable with D₂O, -SO₂NH); ¹³C NMR (DMSO-*d*₆, 100 MHz) δ (ppm): 34.38, 38.89, 114.19 (3C), 116.05 (2C), 119.27 (6C), 124.92, 128.23 (5C), 135.88 (2C), 136.48, 136.62, 140.84, 142.29, 142.62, 143.61, 143.81, 146.73, 151.61, 153.50 (2C), 166.21, and 167.00 (2C); DEPT (DMSO-*d*₆, 100 MHz) δ (ppm): 34.38, 38.89 (2CH₂), 114.21(2), 116.04(2), 116.29(2), 119.28(4), 124.92(2), 128.25(4), 142.62(2), and 143.61(2) (20CH); Anal. calcd. for C₃₅H₂₈N₁₀O₇S₃ (796.13): C, 52.76; H, 3.54; N, 17.58. Found: C, 52.47%; H, 3.22%; N, 17.25%.

4.2 | Biological evaluation

4.2.1 | In vitro antiproliferative activity

Antiproliferative activity screening of the newly synthesized compounds was carried out against three human cancer cell lines namely Hep G-2, Hep-2, and Caco-2. The cell lines were obtained from ATCC (American Type Culture Collection) via the Holding company for biological products and vaccines (Vacsera, Cairo, Egypt). The anti-cancer activity was measured quantitatively using the neutral red assay protocol as described by Borenfreund and Puerner^[41] as follows:

The cell lines were cultured on Dulbecco's modified Eagle Media (DMEM; Lonza) supplemented with 200 mM of L-glutamine and 10% of fetal bovine serum (Gibco-BRL). The test compounds were dissolved in a mixture of dimethyl sulfoxide and DMEM with ratio 4:100 (v/v), respectively. An initial dose of (1 mg/ml) was tested on all cell lines and subsequenced by seven more dilutions using the value of 50% as a dilution factor from the starting dose. The cells were seeded with a concentration of 6×10^4 cell/ml for 24 hr in flat-bottom 96-well plates at 5% CO₂ and 37°C until semiconfluent cell layer was obtained, then, treated with 100 µl of each of serially diluted compounds. After 48 hr, the anticancer activity of the compounds was measured quantitatively by enzyme-linked immunosorbent assay microplate reader at wavelength 540 nm using neutral red assay protocol.

4.2.2 | Measurement of Topo II activity

Twelve compounds that showed high antiproliferative activities (**16**, **18b**, **19b**, **19c**, **22**, **23**, **24a**, **25a**, **25b**, **26**, **27**, and **28b**) were further evaluated to assess their Topo II inhibitory activities. In this test, a Topo II drug screening kit (TopoGEN, Inc., Columbus) was utilized to determine the Topo II activity according to the method described by Ibrahim et al.^[19] Doxorubicin was used as a reference drug in this test.

A typical enzyme reaction contained a mixture of human Topo II (2 µl), substrate supercoiled pHot1 DNA (0.25 µg), 50 µg/ml test compound (2 µl), and assay buffer (4 µl). The reaction started upon incubation of the mixture in 37°C for 30 min. The reaction was terminated by addition of 10% sodium dodecylsulfate (2 µl) and proteinase K (50 µg/ml) at 37°C for 15 min followed by incubation for 15 min at 37°C. Then, the DNA was run on 1% agarose gel in BioRad gel electrophoresis system for 1–2 hr followed by staining with GelRed™ stain for 2 hr and destained for 15 min with TAE buffer (Tris base, acetic acid and EDTA). The gel was imaged via BioRad's Gel Doc™ EZ system. Both supercoiled and linear strands DNA were incorporated in the gel as markers for DNA-Topo II intercalators. The results of IC₅₀ values were calculated using the GraphPad Prism version 5.0. Each reaction was performed in duplicate, and at least three independent determinations of each IC₅₀ were made.

4.2.3 | DNA/methyl green assay

Twelve compounds that exhibited significant antiproliferative activities (**16**, **18b**, **19b**, **19c**, **22**, **23**, **24a**, **25a**, **25b**, **26**, **27**, and **28b**) were further evaluated to determine their DNA-binding affinities. Doxorubicin as a DNA intercalator was used as a positive control. In this test, methyl green dye can bind with DNA to form colored reversible complex of DNA/methyl green. These complexes stay stable at neutral pH. Upon addition of intercalating agents, the methyl green is displaced from DNA with the addition of H₂O molecule to the dye resulting in the formation of the colorless carbinol, leading to a dramatic decrease in spectrophotometric absorbance.^[43] ΔA value

(the difference between DNA/methyl green complex and free carbinol) provides the simplest means for detecting the DNA-binding affinity and relative binding strength. IC₅₀ values were determined using the GraphPad Prism 5.0 software. The reaction was performed as follows.

A mixture of calf thymus DNA (10 mg) and methyl green (20 mg) (Sigma-Aldrich) in 100 ml of 0.05 M Tris-HCl buffer (pH 7.5) containing 7.5 mM MgSO₄. Then, the mixture was stirred for 24 hr at 37°C. The test samples were dissolved in ethanol and dispensed into wells of a 96-well microtiter tray at a concentration of 10, 100 and 1,000 µM. From each well, the excess solvent was removed under vacuum followed by an addition of 200 µl of the DNA/methyl green solution. The test samples were incubated in the dark at an ambient temperature. After 24 hr, the absorbance of each sample was determined at 642.5–645 nm. Readings were corrected for initial absorbance and normalized as the percentage of the untreated DNA/methyl green absorbance value.

4.2.4 | Flow cytometric analysis of cell cycle and apoptosis

According to the method described by Léonce et al.,^[46] flow cytometric analysis was carried out. In this test, PI is used to discriminate between living cells from dead ones or for cell-cycle analysis. The cell-cycle analysis is based on the stoichiometric binding of PI to intracellular DNA. Hep G-2 cells were seeded in 100-mm culture dishes and immediately incubated with the test compound **19b**. After 24 hr, the cells were washed, fixed, and stained in phosphate-buffered saline (PBS), Triton X-100 (0.1%), RNase A (1 mg/ml), and 0.5 ml of PI in PBS (1 mg/ml). Then, the DNA content was determined with a flow cytometer and the distribution of cells in pre-G1 (apoptotic cells), G0/G1, S, and G2/M peaks were quantified by histogram analysis. The obtained data represent three independent experiments.

4.2.5 | Apoptosis using annexin V-fluorescein isothiocyanate (FITC) assay

Further apoptotic effects of compound **19b** against Hep G-2 cells were estimated using an Annexin V-FITC Apoptosis Detection Kit I (Becton Dickinson, Franklin Lakes, NJ) following the manufacturer's protocol. In this test, Hep G-2 cells were treated with compound **19b** (2.5 µg/ml) for 24 and 48 hr. Then, the cells were collected through centrifugation at 2,000 rpm for 5 min. The supernatant was rejected, and the pellets were washed in 100 µl of binding buffer. Next, the cells were incubated for 15 min on ice in the dark with a mixture of 5 µl of PI and 5 µl of annexin V. Then, 400 µl of binding buffer (10 mM 4-(2-hydroxyethyl)-1-piperazineethanesulfonic acid, 140 mM NaCl, and 2.5 mM CaCl₂ at pH 7.4) were loaded and the analysis was completed using a flow cytometer. The untreated cells were considered as negative control.^[47]

4.2.6 | Gene expression analysis (RNA extraction and real-time RT-PCR for tested genes)

According to the manufacturer's protocol, Gene-JET RNA Purification Kit (Thermo Fisher Scientific) was used for extraction of the total RNA from treated and controlled cells. Thermo Scientific cDNA Synthesis Kit was used for the synthesis of complementary DNA (cDNA). The quantification of Bcl-2 and Bax genes was done by real-time PCR using the Maxima SYBR Green/ROX qPCR Master Mix. RT-PCR was performed in a total reaction volume of 25 μ l, which included 2 μ l cDNA, 8 μ l forward and reverse primer, 2.5 μ l nuclease-free water, and 12.5 μ l SYBR green PCR master mix according to the manufacturer's protocol. The thermal cycling protocol of RT was carried out as follows: 50°C for 2 min, 95°C for 15 min, 40 cycles of 15 s at 94°C, 30 s at 50°C, and 30 s at 72°C.^[53] Primer sequences are the following:

Bcl-2 F: 5'-CCTGTGGACTGAGTACC-3'. Bcl-2 R: 5'-GAGACAGCCAGGAGAAATCA-3'.

Bax F: 5'-GTTTCATCCAGGATCGAGCAG-3'. Bax R: 5'-CATCTTCTTCCAGATGGTGA-3'.

4.3 | Molecular docking

4.3.1 | Docking studies

Docking studies were performed using Discovery Studio 4.0, where the binding affinities of the designed compounds against the target macromolecule (DNA-Topo II complex) were evaluated. The three-dimensional (3D) crystal structure of the target complex was retrieved from the Protein data Bank (PDB ID: 4GOU, resolution: 2.7 Å). First, the ligand and water molecules were deleted from the target molecule, leaving only the protein and DNA. Then, the atoms with incorrect valence were corrected using the Valence monitor option. Then, the energy of the DNA-Topo complex was minimized by applying CHARMM and MMFF94 force fields as described in the Supporting Information.^[54-57] The active binding site from the receptor cavity was defined and prepared for docking procedure as described in the Supporting Information. The structures of the synthesized compounds and reference ligands, doxorubicin, and amsacrine (cocrystallized ligand) were sketched using ChemBioDraw Ultra 14.0 and saved in MDL-SD file format. Next, the SD file was opened, 3D structures were protonated and the energy was minimized by applying CHARMM and MMFF94 force fields. The sequence of energy minimization of the designed compounds and the reference ligands was carried out as described in the Supporting Information.

CDOCKER protocol was used for carrying out the docking studies, which employs CHARMM (Chemistry at Harvard Macromolecular Mechanics)-based molecular dynamics scheme to dock ligands into a receptor-binding site. A maximum of 10 conformers was considered for each molecule in the docking analysis. Finally, the most ideal pose was selected according to the minimum free energy of the DNA-Topo II ligand interactions.

ORCID

Ibrahim H. Eissa  <http://orcid.org/0000-0002-6955-2263>

Amany Belal  <http://orcid.org/0000-0003-1045-0163>

Khaled El-Adl  <http://orcid.org/0000-0002-8922-9770>

REFERENCES

- [1] WHO, Cancer, Fact Sheet, 2018 (accessed October 2018). Retrieved from <http://www.who.int/news-room/fact-sheets/detail/cancer>.
- [2] E. Espinosa, P. Zamora, J. Feliu, M. González Barón, *Cancer Treat. Rev.* **2003**, 29, 515.
- [3] L. H. Hurley, *Nat. Rev. Cancer* **2002**, 2, 188.
- [4] J. C. Wang, *Nat. Rev. Mol. Cell. Biol.* **2002**, 3, 430.
- [5] H. Lodish, A. Berk, S.L. Zipursky, P. Matsudaira, D. Baltimore, J. Darnell, *Mol. Cell. Biol.* **2000**.
- [6] W. A. Denny, *Expert Opin. Emerg. Drugs* **2004**, 9, 105.
- [7] Y. Pommier, E. Leo, H. Zhang, C. Marchand, *Chem. Biol.* **2010**, 17, 421.
- [8] M. A. Hogan, D. S. McKinney, in *Comprehensive Review for NCLEX-PN*, 2nd ed., Pearson, New Jersey **2012**.
- [9] B. Kaina, *Biochem. Pharmacol.* **2003**, 66, 1547.
- [10] J. L. Nitiss, *Nat. Rev. Cancer* **2009**, 9, 338.
- [11] R. Martinez, L. Chacon-Garcia, *Curr. Med. Chem.* **2005**, 12, 127.
- [12] L. F. Liu, *Ann. Rev. Biochem.* **1989**, 58, 351.
- [13] A. Chilini, G. Marzaro, C. Marzano, L. D. Via, M. G. Ferlin, G. Pastorini, A. Guiotto, *Bioorg. Med. Chem.* **2009**, 17, 523.
- [14] T. D. Shenkenberg, *Ann. Intern. Med.* **1986**, 105, 67.
- [15] C. Avendano, J. Menéndez, in *Medicinal Chemistry of Anticancer Drugs*, 2nd ed., Elsevier, Amsterdam **2008**, pp. 199-228.
- [16] Y. C. Liaw, Y. G. Gao, H. Robinson, G. A. van der Marel, J. H. van Boom, A. H. J. Wang, *Biochemistry* **1989**, 28, 9913.
- [17] B. A. Armitage, in *DNA Binders and Related Subjects*, Springer, New York **2005**, pp. 55-76.
- [18] S. Takenaka, M. Takagi, *Bull. Chem. Soc. Japan* **1999**, 72, 327.
- [19] M.-K. Ibrahim, A. A. Abd-Elrahman, R. R. A. Ayyad, K. El-Adl, A. M. Mansour, I. H. Eissa, *Bull. Fac. Pharm. Cairo Univ.* **2013**, 51, 101-111.
- [20] M. K. Ibrahim, I. H. Eissa, A. E. Abdallah, A. M. Metwaly, M. M. Radwan, M. A. ElSohly, *Bioorg. Med. Chem.* **2017**, 25, 1496.
- [21] A.-G. A. El-Helby, R. R. A. Ayyad, K. El-Adl, H. Sakr, A. A. Abd-Elrahman, I. H. Eissa, A. Elwan, *Med. Chem. Res.* **2016**, 25, 3030.
- [22] B. Oyallon, M. Brachet-Botineau, C. Logé, P. Bonnet, M. Souab, T. Robert, S. Ruchaud, S. Bach, P. Berthelot, F. Gouilleux, M. C. Viaud-Massuard, C. Denevault-Sabourin, *Eur. J. Med. Chem.* **2018**, 154, 101.
- [23] M. G. Varrica, C. Zagni, P. G. Mineo, G. Floresta, G. Monciino, V. Pistarà, A. Abbadessa, A. Nicosia, R. M. Castilho, E. Amata, A. Rescifina, *Eur. J. Med. Chem.* **2018**, 143, 583.
- [24] Y.-S. Park, W.-S. Shin, C.-S. Kim, C. M. Ahn, X.-F. Qi, S.-K. Kim, *J. Biochem. Mol. Toxicol.* **2018**, 14, 9.
- [25] M. K. Ibrahim, M. S. Taghour, A. M. Metwaly, A. Belal, A. B. M. Mehany, M. A. Elhendawy, M. M. Radwan, A. M. Yassin, N. M. El-Deeb, E. E. Hafez, M. A. ElSohly, I. H. Eissa, *Eur. J. Med. Chem.* **2018**, 155, 117.
- [26] W. M. Eldehna, M. F. Abo-Ashour, A. Nocentini, P. Gratteri, I. H. Eissa, M. Fares, O. E. Ismael, H. A. Ghabbour, M. M. Elaasser, H. A. Abdel-Aziz, C. T. Supuran, *Eur. J. Med. Chem.* **2017**, 139, 250.
- [27] A. A. Gaber, A. H. Bayoumi, A. M. El-Morsy, F. F. Sherbiny, A. B. M. Mehany, I. H. Eissa, *Bioorg. Chem.* **2018**, 80, 375.
- [28] A. M. El-Naggar, M. M. Abou-El-Regal, S. A. El-Metwally, F. F. Sherbiny, I. H. Eissa, *Mol. Divers.* **2017**, 21, 967.
- [29] S. A. Elmetwally, K. F. Saied, I. H. Eissa, E. B. Elkaeed, *Bioorg Chem.* **2019**, 88, 102944.

- [30] I. H. Eissa, A. M. El-Naggar, M. A. El-Hashash, *Bioorg. Chem.* **2016**, *67*, 43.
- [31] I. H. Eissa, A. M. El-Naggar, N. E. A. A. El-Sattar, A. S. A. Youssef, *Anticancer Agents Med. Chem.* **2018**, *18*, 195.
- [32] D. E. Graves, L. M. Velea, *Curr. Org. Chem.* **2000**, *4*, 915.
- [33] F. Gago, *Methods* **1998**, *14*, 277.
- [34] G. Minotti, P. Menna, E. Salvatorelli, G. Cairo, L. Gianni, *Pharmacol. Rev.* **2004**, *56*, 185.
- [35] J. Gallego, A. R. Ortiz, B. Pascual-Teresa, F. Gago, *J. Comp. Aided Mol. Des.* **1997**, *11*, 114.
- [36] S. A. Bailey, D. E. Graves, R. Rill, *Biochemistry* **1994**, *33*, 11493.
- [37] P. Traxler, P. Furet, *Pharmacol. Ther.* **1999**, *82*, 195.
- [38] D. R. Romer, *J. Heterocyclic Chem.* **2009**, *46*, 317.
- [39] K. Sarges, H. R. Howard, R. G. Browne, L. A. Lebel, P. A. Seymour, B. K. Koe, *J. Med. Chem.* **1990**, *33*, 2240.
- [40] M. Alswah, A. Ghiaty, A. El-Morsy, K. El-Gamal, *ISRN Org. Chem.* **2013**, *2013*, 1.
- [41] E. Borenfreund, J. A. Puerner, *Toxicol. Lett.* **1985**, *24*, 119.
- [42] P. Furet, G. Caravatti, N. Lydon, J. P. Priestle, J. M. Sowadski, U. Trinks, P. Traxler, *J. Comp. Aided Mol. Des.* **1995**, *9*, 465.
- [43] N. S. Burres, A. Frigo, R. R. Rasmussen, J. B. McAlpine, *J. Nat. Prod.* **1992**, *55*, 1582.
- [44] S. W. Lowe, A. W. Lin, *Carcinogenesis* **2000**, *21*, 485.
- [45] C. Riccardi, I. Nicoletti, *Nat. Protoc.* **2006**, *1*, 1458.
- [46] S. Léonce, V. Pérez, S. Lambel, D. Peyroulan, F. Tillequin, S. Michel, M. Koch, B. Pfeiffer, G. Atassi, J. A. Hickman, A. Pierré, *Mol. Pharmacol.* **2001**, *60*, 1383.
- [47] K. K.-W. Lo, T. K.-M. Lee, J. S.-Y. Lau, W.-L. Poon, S.-H. Cheng, *Inorg. Chem.* **2008**, *47*, 200.
- [48] Y. Tsujimoto, C. M. Croce, *Proc. Natl. Acad. Sci. USA* **1986**, *83*, 5214.
- [49] J. Pawlowski, A. S. Kraft, *Proc. Natl. Acad. Sci. USA* **2000**, *97*, 529.
- [50] D. Westphal, R. M. Kluck, G. Dewson, *Cell Death Differ.* **2014**, *21*, 196.
- [51] A. Kumar, U. Bora, *Interdiscip. Sci.: Comp. Life Sci.* **2014**, *6*, 285.
- [52] I. H. Eissa, A. M. El-Naggar, N. E. A. A. El-Sattar, A. S. A. Youssef, *Anticancer Agents Med. Chem.* **2018**, *18*, 195.
- [53] K. J. Livak, T. D. Schmittgen, *Methods* **2001**, *25*, 402.
- [54] A. G. A. El-Helby, R. R. Ayyad, H. M. Sakr, A. S. Abdelrahim, K. El-Adl, F. S. Sherbiny, I. H. Eissa, M. M. Khalifa, *J. Mol. Struct.* **2017**, *1130*, 333.
- [55] M. K. Ibrahim, I. H. Eissa, M. S. Alesawy, A. M. Metwaly, M. M. Radwan, M. A. ElSohly, *Med. Chem.* **2017**, *25*, 4723.
- [56] K. M. El-Gamal, A. M. El-Morsy, A. M. Saad, I. H. Eissa, M. Alswah, *J. Mol. Struct.* **2018**, *1166*, 15.
- [57] M. A. El-Zahabi, E. R. Elbendary, F. H. Bamanie, M. F. Radwan, S. A. Ghareib, I. H. Eissa, *Bioorg. Chem.* **2019**, *91*, 103115.

SUPPORTING INFORMATION

Additional supporting information may be found online in the Supporting Information section.

How to cite this article: Eissa IH, Metwaly AM, Belal A, et al. Discovery and antiproliferative evaluation of new quinoxalines as potential DNA intercalators and topoisomerase II inhibitors. *Arch Pharm Chem Life Sci.* 2019;e1900123. <https://doi.org/10.1002/ardp.201900123>